JOURNAL OF SPACECRAFT AND ROCKETS
Vol. 30, No. 4, July–August 1993

Shuttle Entry Aerothermodynamic Flight Research: The Orbiter Experiments Program

David A. Throckmorton*
NASA Langley Research Center, Hampton, Virginia 23681

Routine operations of the nation's Space Transportation System have provided recurring opportunities for aerothermodynamicists to study entry aerothermal phenomena unique to lifting entry vehicles in hypersonic flight. Initiated in the mid-1970s, the Orbiter Experiments (OEX) Program provided a mechanism for utilization of the Shuttle Orbiter as an entry research vehicle as an adjunct to its normal operational mission. The data derived from OEX Program experiments represent benchmark hypersonic flight results heretofore unavailable for a lifting entry vehicle. These data are being used in a continual process of validation of state-of-the-art methods, both experimental and computational, for simulating and/or predicting the aerothermodynamic flight characteristics of advanced space transportation vehicles. The OEX Program complement of research experiments is described, typical flight data obtained by these experiments are presented, and utilization of these data for validation of advanced vehicle aerothermodynamic design tools is demonstrated.

Nomenclature

L/D	=lift-to-drag ratio
q	=heat transfer rate, kW/m^2
R_{NS}	=normal shock Reynolds number
St	=Stanton number
x/L	=nondimensional vehicle length, L=32.77 m
X, Y, Z	=Orbiter geometric coordinates, cm
ρ/ρ_{76}	=nondimensional density, relative to 1976 standard atmosphere

Introduction

THE NASA Orbiter Experiments (OEX) Program had its genesis in the early days of the Space Shuttle Program's Phase C/D, design and development of the Shuttle Orbiter. Development of the Orbiter represented the first attempt to design a reusable vehicle capable of controlled aerodynamic entry from low-Earth orbit to a horizontal landing at a predetermined landing site. The operational requirements of this vehicle presented significant challenges to its aerothermodynamic designers. The vehicle was required to be aerodynamically controllable across the speed regime, from Earth-orbital, hypersonic entry velocities to low subsonic landing speeds; and the vehicle's thermal protection system (TPS) was required to protect the vehicle's structure from the extreme levels of aerodynamic heating that would accompany the hypersonic entry, yet be reusable for many additional missions.

The aerothermodynamic design process required a high degree of integration among the disciplines of aerodynamics, aeroheating, and guidance, navigation, and control (GN&C). The aerodynamic performance and stability and control characteristics of the Orbiter configuration had to be adequately defined over the entire entry flight regime to enable design of the guidance, navigation, and flight control systems. The vehicle's aerodynamic heating environment had to be adequately predicted to enable design of the thermal protection system, as well as definition of the thermal flight envelope constraints that would influence entry trajectory design.

Presented as Paper 92-3987 at the AIAA 17th Aerospace Ground Testing Conference, Nashville, TN, July 6–8, 1992; received Oct. 5, 1992; revision received Nov. 27, 1992; accepted for publication Nov. 27, 1992.

*Assistant Head, Aerothermodynamics Branch, Space Systems Division.

An extensive program of ground-based testing was undertaken to generate the database required for the aerothermodynamic design of the Orbiter vehicle. This test program, which required tens of thousands of hours of testing in the nation's hypersonic wind-tunnel facilities, included aerodynamic performance, stability and control, and aerodynamic heat transfer testing. This expansive ground-test program notwithstanding, it was recognized that before the Orbiter's first flight, significant uncertainties would exist in predictions of both the vehicle's aerodynamic characteristics and its aerodynamic heating environment. These uncertainties resulted from inherent limitations in the ability of ground-test facilities to adequately simulate the full-scale flight environment. Although existing test facilities could, in some instances, replicate certain of the relevant parameters (e.g., Mach number or Reynolds number), no facility could provide simultaneous simulation of all of the relevant parameters. More importantly, no facilities existed that could replicate the real-gas aspects of the flight environment. Additionally, since no data existed for a lifting vehicle in the actual flight environment, methodologies for extrapolation of ground-test results to the flight environment could not be validated.

The vehicle's flight control and thermal protection system designs were required to be sufficiently robust to assure fail-safe operation of the Orbiter during entry in the face of these uncertainties. Systems' robustness would be obtained through the application of significant factors of conservatism in the systems' designs. This conservatism would result in a highly constrained aerodynamic flight envelope, in severe limitations on allowable vehicle center-of-gravity variation, and most probably in an overweight thermal protection system.

The conservatism in the Orbiter's aerothermodynamic design was known to be significant, and the research community recognized the importance of eliminating this conservatism in the design of future entry vehicles. Members of this community also recognized the unique opportunity that Shuttle operations might provide: to routinely gather hypersonic aerothermodynamic flight data with which to enhance understanding of the real-gas, hypersonic flight environment and to enable improvement and validation of ground-to-flight data extrapolation techniques. Thus the concept of the OEX Program was born.

Orbiter Experiments Program

The concept of utilizing the Shuttle Orbiter as a flight research vehicle, as an adjunct to its normal operational mission, was a topic of discussion within the research community circa 1974. In this time frame, the idea received programmatic attention in deliberations of the NASA Research and Technology Advisory Coun-

cil's (RTAC) Panel on Space Vehicles. Meetings of this panel in March and October of 1975 resulted in recommendations to the NASA Office of Aeronautics and Space Technology (OAST) that it pursue development and implementation of expanded flight-test instrumentation to be flown aboard the Shuttle Orbiter.

Potential flight investigations were identified and/or documented during a space technology workshop sponsored by the NASA OAST in August 1975.[1] This workshop was intended 1) to foster identification of areas of needed technology development that required, or could substantially benefit from, space flight experimentation and 2) to define candidate flight research experiments that would address those technology development needs by taking advantage of the ready access to space that was to become possible with the advent of Shuttle operations. Entry technology was one of 11 research areas addressed at this workshop. The report of the workshop's Entry Technology Panel[2] included recommendations of specific flight instrumentation concepts that, if implemented, would enable collection of aerothermodynamic flight research data during atmospheric entry of the Shuttle Orbiter. A subsequent Mini-Workshop on entry technology in March 1976 provided for more detailed definition of candidate flight experiments.

These preliminary planning activities, as well as the deliberations and recommendations of the RTAC Panel on Space Vehicles, led to the establishment in July 1976 of the OEX Program. Initial funding for the program was provided, for fiscal year 1977, from discretionary funds of the associate administrator of OAST. The OEX Program was an integral part of the proposed NASA budget for fiscal year 1978. As such, the program was discussed in testimony (see Ref. 3) before congressional committees with NASA oversight, during the fiscal year 1978 budget authorization process. The OEX Program was approved as part of the NASA budget and began to receive yearly funding allocations in fiscal year 1978.

Aerothermodynamic Flight Research Data Requirements

Performing aerothermodynamic research in the hypersonic flight environment is not unlike the process of conducting similar research in ground-based wind-tunnel facilities. The generic data requirements of both are identical, although the manner in which those data are obtained may differ. In both instances, the freestream environment in which the test is being conducted must be characterized, and the vehicle's attitude with respect to the freestream must be accurately known. For aerodynamic testing, the aerodynamic forces acting on the vehicle must be determined; and for aerothermal testing, aerodynamic surface pressure, temperature, and heat transfer rate data must be obtained. Of course, in both instances, the vehicle's aerodynamic configuration (i.e., control surface deflection positions) must also be known.

Table 1 presents a summary list of the classes of data required for the determination of hypersonic vehicle aerothermodynamic characteristics, whether testing is performed in ground-based wind-tunnel facilities or in flight. The measurement techniques used to obtain these data in flight are compared with those used to obtain similar data in the wind tunnel. The following subsections contain more in-depth discussions of these data classes and the contrasting flight vs wind-tunnel data measurement techniques.

Table 1 Aerothermodynamic measurement techniques comparison

	Measurement technique	
Data class	Wind tunnel	Flight
Freestream environment definition	Facility calibration	Atmospheric soundings
	Total and/or static pressure and temperature measurements	Air-data system
Vehicle attitude	Specified and controlled	Air-data system Inertial data
Aerodynamic forces and moments	Force balance	Linear and angular accelerations and rate measurements Mass and moments-of-inertia tracking
Surface conditions	Direct measurement	Direct measurement
Configuration	Specified and controlled	Direct measurement

Freestream Environment and Vehicle Attitude Data

Freestream environmental definition in hypersonic wind-tunnel facilities is typically achieved through a combination of facility calibration and direct measurement of pertinent flow variables. Stream total temperature (or enthalpy) and total pressure are normally measured directly during a test. The total temperature and pressure information are often obtained within the facility settling chamber, upstream of the hypersonic nozzle. When combined with an accurate facility calibration, these data enable determination of the pertinent flow parameters (e.g., freestream static pressure and temperature, dynamic pressure, and Mach and Reynolds numbers) that characterize the test environment. Vehicle attitude parameters (i.e., angles of attack and sideslip) are, of course, specified and controlled test variables.

In flight testing, the freestream environment is similarly characterized by the measurement of appropriate flight-test variables, which enable determination of the pertinent freestream flow parameters. Normally, a calibrated "air-data" probe is mounted at the end of a long boom attached to the nose of the flight-test vehicle to enable direct, in situ measurements of freestream dynamic and static pressures, freestream total temperature, and vehicle attitude during flight testing. If for some reason an air-data boom cannot be used, alternate (less accurate) approaches may be implemented to infer the required environmental data. Atmospheric properties of static temperature, pressure, density, and winds may be determined as a function of altitude by balloon-borne measurement devices; and vehicle position (altitude) and velocity (ground relative) may be determined by ground-based radar tracking. Inertial measurement devices onboard the test vehicle may also be used for the determination of vehicle velocity and attitude (relative to an inertial reference, without respect to winds).

Aerodynamic Force and Moment Data

Aerodynamic force and moment measurements in hypersonic wind tunnels are normally obtained in a straightforward manner using six-component force balances. These devices provide for direct measurements of the forces and moments acting on the test model through the moment center of the installed balance. The measured force and moment data need only be corrected to account for the effects of base pressure, which may be influenced by the presence of the support sting, and translation of moments to an assumed configuration center-of-gravity position.

Flight-test determinations of aerodynamic forces and moments are accomplished by measurement of the three-axis linear accelerations and angular accelerations and rates experienced by the vehicle in flight. These data, when combined with appropriate vehicle mass, center-of-gravity, and moments-of-inertia information, enable determination of the in-flight aerodynamic forces and moments.

Aerodynamic coefficients and stability and control derivatives are determined from flight-measured dynamic data using a process known as "maximum-likelihood estimation." In the maximum-likelihood estimation process,[4] the six-degree-of-freedom equations of motion are formulated with vehicle aerodynamic coefficients and stability and control derivatives, as independent model variables. In flight, a precisely defined vehicle aerodynamic control input is commanded and measured, and the resulting small-perturbation vehicle dynamic response data are recorded. The vehicle's estimated (expected) response to the control input (based on the preflight aerodynamic model) is then compared with the actual measured response. Based on this comparison, the aerodynamic model is updated, and a new vehicle response estimate is generated, which is again compared with the measured response. This process is performed iteratively until the differences between the estimated and actual response data are statistically minimized. The resulting aerodynamic model then represents the maximum-

Table 2 Shuttle flight instrumentation summary

	Flight environment	Vehicle motion	Vehicle surface	Vehicle configuration
	Altitude dependent		All altitude	
		ACIP and IMU		
	SEADS		DFI and AIP	
Increasing altitude			TGH and CSE	OI[a]
		HiRAP		
			IRIS and SILTS	
	SUMS			
		OARE		

[a]OI = operational instrumentation.

likelihood estimate of the vehicle's in-flight aerodynamic characteristics.

Aerodynamic Surface Data

Methods used to obtain aerodynamic surface data in flight and those used in hypersonic wind tunnels are fundamentally identical. The specific implementation approaches may differ somewhat, however, because of the unique characteristics of the differing environments in which the measurement devices are required to operate.

Pressure

Hypersonic wind-tunnel measurements of surface pressure data are normally obtained using complex models that contain tens, or possibly hundreds, of small orifices normal to the aerodynamic surface through which static pressure may be sensed. Usually, each orifice is individually connected by tubes that extend through the model support structure to the outside of the wind-tunnel test section to a pressure measurement device. Good engineering practice demands that tube lengths between orifices and sensors be minimized. However, if this is not possible, in a wind-tunnel facility, pressure losses due to tube length may still be accounted for through proper system calibration, and/or the wind-tunnel test may be designed to assure that the measured pressures are steady state and are not influenced by transient phenomena.

In-flight measurements of surface pressure are similarly obtained with pressure orifices at the aerodynamic surface connected by tubes to individual pressure transducers. Unlike the wind tunnel, however, the flight-test environment (certainly that of the Shuttle Orbiter) is by its very nature a somewhat transient environment. Consequently, care must be taken in the implementation of a flight pressure sensing system to minimize measurement sensitivity to transient phenomena. This is accomplished by locating the pressure transducers as close as is practically possible to their orifice location to minimize tube length. Thus, the influences of both pressure transients and tube losses are minimized.

Heat Transfer Rate

Several techniques are commonly used to measure aerodynamic heat transfer rates in hypersonic wind tunnels. These techniques include the use of models fabricated from solid ceramic material with thin-film gauges installed at the aerodynamic surface, thin-skin metallic models with thermocouples installed at the backface of the metallic sheet, and solid models fabricated of low-conductivity, castable materials with temperature-sensitive (phase-change) paints applied to the surface during a test. Remote-sensing techniques using infrared radiation and thermographic phosphor emissions from the surfaces of solid, noninstrumented models may also be used. In each of these techniques, an isothermal model is rapidly injected into the hypersonic stream and the surface rates of change of temperature with time are determined. These data, when combined with proper modeling of the heat conduction process within the model, enable determination of aerodynamic heat transfer rates.

Techniques for flight measurement of aerodynamic heat transfer rates are analogous to those used in hypersonic wind tunnels. On the Shuttle Orbiter, temperatures within the Orbiter's thermal protection materials were measured at discrete locations by means of in situ thermocouples and/or resistance temperature devices (RTDs). Where installation of these devices was incompatible with the material in which the measurement was to be made, or where spatially continuous temperature distribution data were desired and a vantage point for surface viewing was available, radiometers provided for nonintrusive measurement of temperature levels. As with the wind-tunnel test techniques, when combined with proper modeling of the heat conduction process within the thermal protection materials and reradiation of energy into space (unique to the flight case), these temperature data enabled determination of aerodynamic heat transfer rates to the Orbiter surfaces.

It should be noted that there is a fundamental difference between flight- and wind-tunnel-derived aerodynamic heat transfer rate data. Wind-tunnel data are typically obtained at *isothermal* wall conditions. In flight, however, the wall conditions that exist at any point on the trajectory are the integrated result of the flight environments previously traversed from orbit to that point in time. Therefore, the flight-derived data are obtained at *nonisothermal* wall conditions.

Vehicle Configuration Data

Proper interpretation of aerothermodynamic data from either wind-tunnel or flight tests obviously requires accurate knowledge of the aerodynamic configuration under test. In the context of this discussion, the phrase "configuration data" refers not simply to the geometric shape of the configuration but more specifically refers to the control surface position configuration. In hypersonic wind-tunnel tests, control surface configuration is generally a specified and controlled parameter set.

In flight, control surface positions may or may not be controllable test variables. Specifically in the Shuttle Orbiter case, control surface deflections are first dictated by vehicle trim requirements and the guidance and navigation requirements of the entry trajectory. Variability of the Orbiter's control surface configuration about the nominal is severely limited, constrained by the energy management requirements of the specific entry (the Orbiter is an unpowered glider) and possible thermal constraints on control surface deflection or vehicle attitude. Additionally, nominal control surface positions may differ from mission to mission as a result of mission-dependent vehicle center-of-gravity variations. Nonetheless, control surface position data are measured during Orbiter entry.

As a hybrid spacecraft and aircraft, the Shuttle Orbiter has not only aerodynamic control surfaces but also a reaction control system (RCS) that provides on-orbit vehicle attitude control. The RCS includes some 19 primary and 4 vernier pitch-axis thrusters and 12 primary and 2 vernier yaw-axis thrusters. The RCS is active during much of the hypersonic portion of atmospheric entry, providing attitude control at flight conditions where the dynamic pressure is insufficient for effective attitude control by the aerodynamic control surfaces. Reaction control system operation data are also measured during entry.

OEX Experiment Complement and Operational History

Under the auspices of the OEX Program, various experiment systems were designed, developed, and integrated aboard the Shuttle Orbiter Columbia to enable collection of research-quality aerothermodynamic flight data. Unique OEX experiment instrumenta-

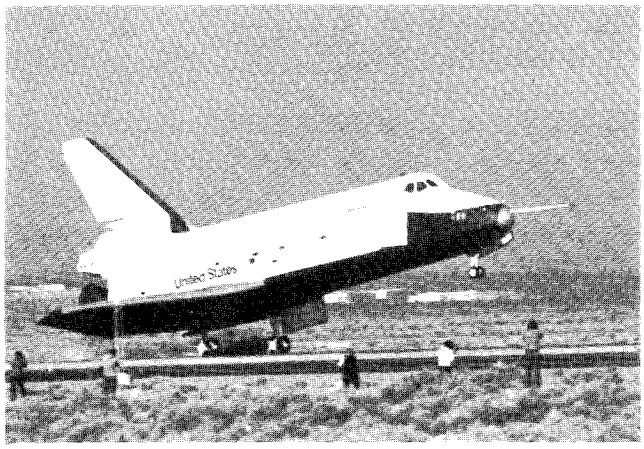

Fig. 1 Orbiter Enterprise during approach and landing test flight.

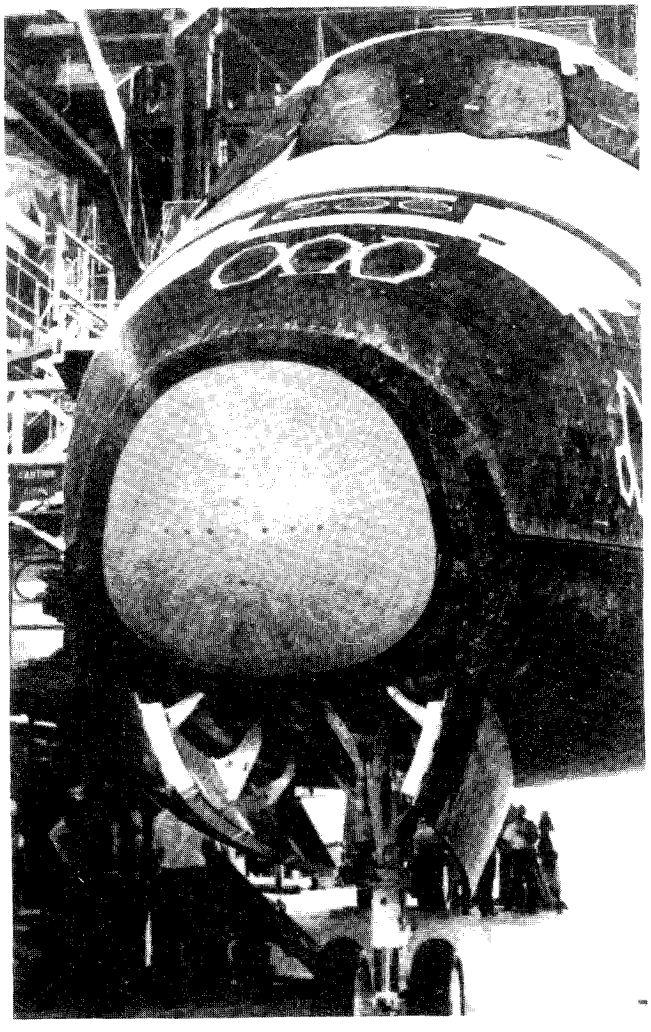

Fig. 2 SEADS nosecap installed on Orbiter Columbia.

tion augmented existing Orbiter instrumentation systems. The total complement of Orbiter instrumentation and OEX experiments comprised a comprehensive instrumentation system for the determination of Orbiter aerodynamic and aerothermal flight characteristics across the entire entry flight regime.

Several early papers[5–7] documented the planning for utilization of the Orbiter as an entry flight research vehicle. Reference 5 provides an excellent presentation of the data requirements for Orbiter aerodynamic testing, as well as descriptions of the Orbiter baseline and OEX measurement systems that were to be implemented to enable Orbiter aerodynamic research. A summary discussion of the more significant Orbiter entry aerothermodynamic problems and short overview descriptions of the proposed OEX experiments are contained in Ref. 6. Lastly, planned aerothermodynamic flight research analyses, to be conducted by NASA Langley Research Center staff members using data obtained during the Orbital Flight Test missions of the Orbiter Columbia, are described in Ref. 7. That paper also contains the first published Orbiter aerodynamic heat transfer data, obtained on the STS-1 mission entry.

The following subsections contain discussions of both the Orbiter baseline and OEX-unique experiment systems that were incorporated (and/or used) for the purpose of obtaining Orbiter entry aerothermodynamic flight research data. These discussions are organized by data type, in the same manner as the foregoing section. Each experiment system discussion addresses the experiment concept, its hardware implementation, and its flight operational performance history. Table 2 presents a summary of the specific instrumentation systems used, categorized by data type and the flight regime of system operation.

Freestream Environment and Vehicle Attitude Data

The Shuttle Orbiter Enterprise was equipped with an air-data boom to obtain freestream environment and vehicle attitude data during the Orbiter's Approach and Landing Test Program (Fig. 1). At hypersonic speeds, however, utilization of an air-data boom is not practical because of the extreme aerodynamic heating environment that accompanies hypersonic flight. Consequently, a nonintrusive method of measuring air-data parameters is required for a hypersonic flight-test vehicle. The challenge of obtaining air data on a hypersonic flight vehicle was first faced during the X-15 program. That vehicle incorporated a spherical "ball-nose" flow direction sensor.[8] This sensor used differential pressure measurements from orifices located on opposite sides of a sphere at the vehicle's nose to drive a hydraulic actuator that rotated the sphere so as to null the pressure differential. The resulting position of the sphere relative to the vehicle centerline provided a direct indication of angles of attack and sideslip. The ball nose also contained a stagnation-point pressure orifice. Although not used for the purpose at the time, this pressure measurement could have been used for determination of freestream dynamic pressure.

For Shuttle Orbiter *operational* purposes, inertial measurement techniques are used to infer the air-data parameters required for vehicle GN&C during hypersonic flight. The inertially derived parameters are sufficiently accurate to enable the GN&C system to guide the vehicle to the vicinity of the landing site, where data

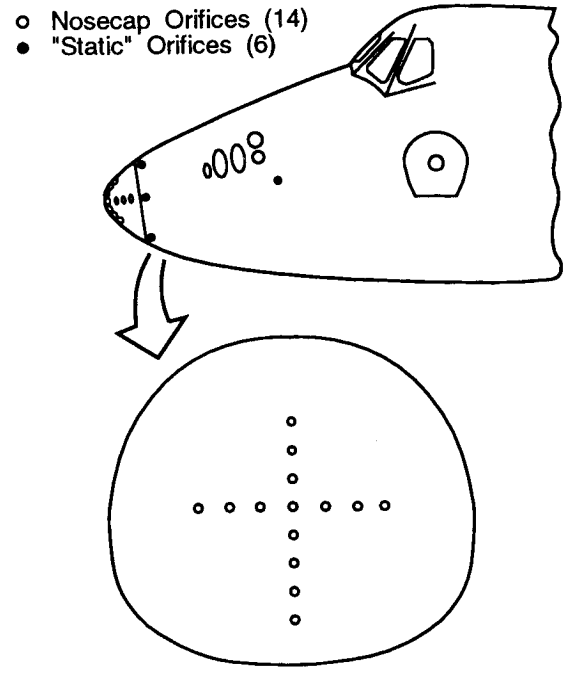

Fig. 3 SEADS orifice location schematic.

from other sources [e.g., tactical air navigation (TACAN), beginning at an altitude of about 49 km] provide updates to the vehicle state vector and enable the vehicle to be flown to a precise landing. The inertially derived air-data parameters are *not* sufficiently accurate, however, for research flight data analyses. Consequently, the OEX Program provided for the development and implementation of both in situ measurement systems and postflight data analysis methods to enable research-quality determination of vehicle freestream environmental and attitude information.

Shuttle Entry Air Data System

The Shuttle Entry Air Data System[9,10] (SEADS) was designed to provide "across-the-speed-range" air data from approximately 90 km altitude, when the Orbiter is traveling in excess of Mach 25, through the supersonic, transonic, and subsonic portions of the entry, to landing. This system might be viewed as *conceptually* similar to the X-15 ball nose; however, its implementation approach is substantially different from, and its air-data parameter determination capability far exceeds, that of the X-15 ball nose. The SEADS system comprised a specially designed Orbiter nosecap, which incorporated 14 pressure-orifice assemblies through which the aerodynamic surface pressure could be measured during entry (Fig. 2). Measurement of the magnitude and distribution of aerodynamic pressure acting on the Orbiter's nosecap in flight enabled accurate postflight determination of vehicle angles of attack and sideslip, as well as freestream dynamic pressure.

The SEADS pressure orifices were arranged in a cruciform array (Fig. 3) with eight orifices in the plane of symmetry and six orifices in the transverse plane. The symmetry-plane orifice array contributed primarily to determination of stagnation point location and pressure and vehicle angle of attack. The transverse orifice array contributed primarily to determination of angle of sideslip. Each orifice assembly was connected, through internal nosecap plumbing, to two pressure transducers, one with a measurement range of 0–1 psia and one with a measurement range of 0–20 psia. Dual range measurements at each orifice assured accurate determination of pressure level for the entire altitude regime over which the system was designed to operate. Temperatures of the pressure transducer banks (of which there were two) were measured to account for the temperature dependence of transducer calibrations. Analog-to-digital conversions of transducer output signals were performed by a 12-bit pulse code modulation (PCM) unit. The data were sampled at a rate of 28 Hz and were recorded on an OEX-dedicated flight data recorder.

The 14 nosecap orifices were augmented by six supplementary orifices located on the Orbiter forebody aft of the nosecap (Fig. 3). Four of these measurements were obtained at locations around the periphery and just aft of the nosecap: two located windward and leeward on the plane of symmetry and one located on either side of the fuselage. Two additional pressure orifices, located well aft of the nose on either side of the fuselage, provided static-pressure data that were of particular importance for low supersonic and subsonic air-data parameter determination.

Air-data parameters were determined from the SEADS pressure data after flight by application of a unique data-processing algorithm. This algorithm incorporated a mathematical model of the pressure distribution about the Orbiter forebody as a function of an aerodynamic state vector that had elements of total and static pressure and angles of attack and sideslip. The mathematical model was constructed based on a combination of theoretical considerations and the results of extensive wind-tunnel tests. The flight-observed pressures were smoothed with respect to time and then "fit" to the model pressures using a digital batch filter process that optimized the aerodynamic state vector by minimizing, in a weighted least squares sense, the differences between the flight-observed and model pressures. The resulting aerodynamic state vector, containing the basic air-data information, was derived at an effective data rate of 4 Hz.

The SEADS was installed in place of the baseline nosecap on the Orbiter Columbia during that Orbiter's modification period in 1984–85. The SEADS was subsequently operated successfully on five Columbia missions: STS-61C, -28, -32, -35, and -40.

Shuttle Upper Atmosphere Mass Spectrometer

The Shuttle Upper Atmosphere Mass Spectrometer (SUMS) experiment[11] was intended to supplement the SEADS by providing atmospheric density data at altitudes above 90 km. Just as SEADS would provide flight environmental information in the continuum-flow flight regime, the SUMS would provide similar data to enable aerodynamic research in the transitional- and free-molecular-flow flight regimes. At these extreme altitudes, aerodynamic surface

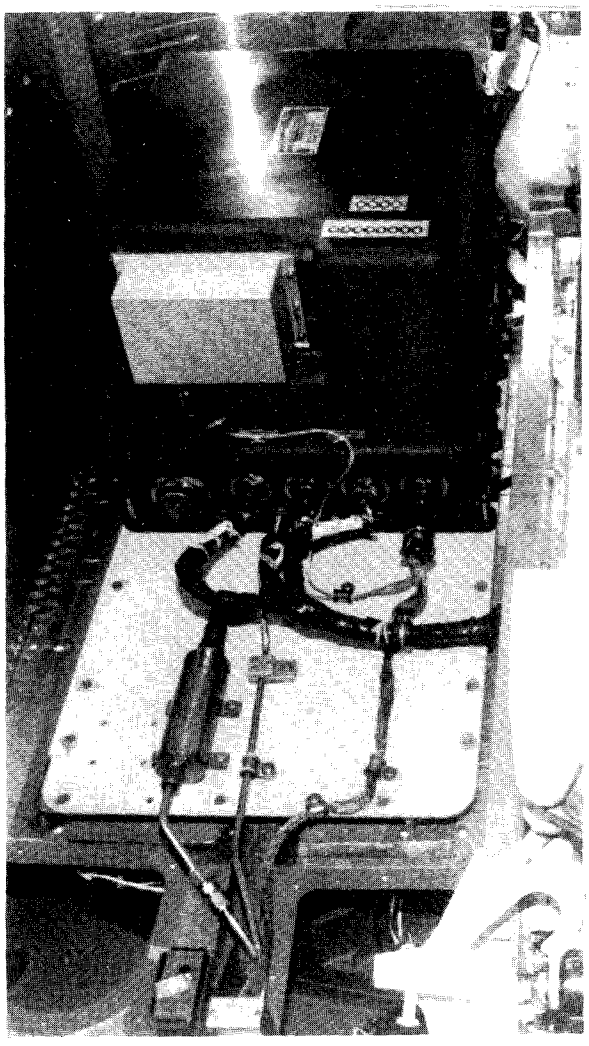

a) Photograph

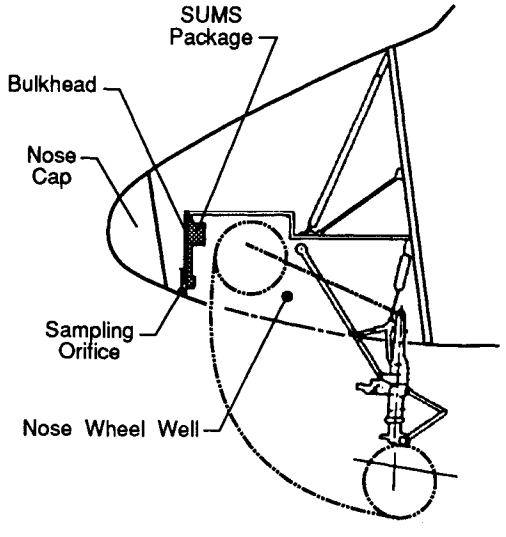

b) Schematic

Fig. 4 SUMS installation in Orbiter Columbia.

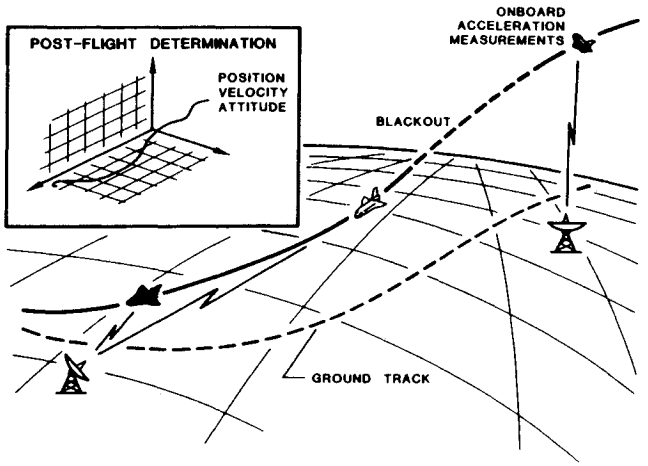

Fig. 5 Entry trajectory reconstruction.

pressures are too low to be accurately sensed by conventional pressure transducers such as those used by the SEADS. Instead, the SUMS instrument used a mass spectrometer, operating as a pressure-sensing device, to determine Orbiter stagnation region surface pressure and then to infer the atmospheric density in this high-altitude, rarefied-flow flight regime.

The SUMS mass spectrometer was originally spare flight equipment developed for the Viking Mars Lander. This mass spectrometer was modified to enable it to operate in the entry flight environment of the Shuttle Orbiter. The SUMS sampled atmospheric gases through an orifice on the Orbiter's lower surface centerline just aft of the Orbiter nosecap; this orifice was shared with the SEADS experiment. The mass spectrometer was connected to the gas-sampling orifice by a unique inlet system comprised of tubing, operation control valves, and a pressure transducer. The SUMS instrument assembly was mounted on the forward bulkhead of the Orbiter's nose wheel well (Fig. 4), with the inlet system connected to the orifice plumbing.

SUMS data were sampled at an effective rate of 0.2 Hz, and recorded on the OEX recorder for postflight processing. The processed SUMS data were combined with computational modeling of the rarefied flow, within both the inlet system and the Orbiter's forebody flowfield,[12] to enable determination of the freestream atmospheric density.

The SUMS was initially installed aboard the Orbiter Columbia following its 1984–85 modification period. The experiment was subsequently flown on STS-61C. Unfortunately, a "protection" valve, designed to prevent atmospheric pressure gases from entering the mass spectrometer during ground operations, failed to open as planned when the vehicle reached orbit and remained stuck in the closed position throughout the mission. Consequently, no freestream gases were able to reach the mass spectrometer during entry and thus no scientific data were obtained on the STS-61C mission. The SUMS was next flown on mission STS-35, during which the system operated properly, gathering data over the altitude range from orbit to 87 km. Useful scientific data were obtained over the approximate altitude range of 172-87 km. Scientific data for altitudes in excess of 172 km were masked by a "background" signal that resulted from gas molecules trapped in the SEADS and SUMS pressure transducers connected to the SUMS inlet system. The last flight of SUMS was on mission STS-40. On this mission, the instrument experienced an automatic shutdown immediately upon experiment initiation. The shutdown occurred (to protect the mass spectrometer from damage) when an excessive pressure level was detected in the mass spectrometer. The excessive pressure was attributed to the vapor pressure of water, which was present in the inlet system at launch. No scientific data were obtained on the STS-40 flight.

Best Estimate of Trajectory

In the absence of the SEADS and SUMS instruments to provide in situ measurements of flight environmental information, these data were determined through processes of "reconstruction" of both the Orbiter entry trajectory and the atmosphere at the time of entry and correlation of these two data sets to provide an analytically and physically consistent best estimate of the entry flight environmental parameters.

The trajectory reconstruction process[13] uses ground tracking data and onboard measurements of Orbiter inertial attitude, linear accelerations, and angular rates to determine the vehicle inertial state vector (inertial position, velocity, and attitude) from near-orbital altitude to landing (Fig. 5). Linear acceleration and angular rate information, derived from Orbiter inertial measurement unit data, are used to deterministically integrate the six-degree-of-freedom equations of motion in time, from a known initial condition (shortly after the de-orbit burn) through Orbiter landing, to define a first estimate of the history of the inertial state vector. These inertial position and velocity estimates are then constrained to fit, in a weighted least squares of residuals sense, the observed position and velocity data measured by the ground-based tracking. The result is a statistically best estimate of the vehicle entry trajectory (position, velocity, and attitude) in an inertial reference space.

Consideration of the rotation and oblate shape of the Earth allows the trajectory information to be transformed into an Earth/atmosphere referenced system. The final product of the trajectory reconstruction process is then a best estimate of the time history of Orbiter position (altitude above an oblate spheroid, latitude, and longitude) and atmosphere-relative (no winds) velocity and attitude (angles of attack and sideslip), from near-orbital altitude to touchdown.

Definition of the state of the atmosphere through which the Orbiter has flown is accomplished by a process[14] that combines atmospheric modeling with direct measurements of atmospheric profiles of pressure, temperature, density, and winds (Fig. 6). Atmospheric soundings made near the time of entry provide the measured atmospheric profiles. However, the soundings are made at only a few locations. These locations may not be along the Orbiter's entry ground track, and the time at which the soundings were made may not correspond well with that of Orbiter entry. Additionally, the soundings only provide measured data to an altitude of approximately 90 km. Atmospheric data above 90 km are estimated using upper atmospheric models to propagate the pressure, temperature, density, and winds data to higher altitudes.

The measured and estimated data are then used to define freestream pressure, temperature, density, and winds along the Orbiter entry corridor. The reconstructed trajectory defines the time of day and corresponding latitude, longitude, and altitude of the Orbiter's entry. Atmospheric modeling is used to define the time of day and latitude variations in atmospheric properties. The measured atmospheric data are extrapolated to the Orbiter entry corridor in a manner that accounts for the time of day and latitude differences between the Orbiter entry and the atmospheric soundings.

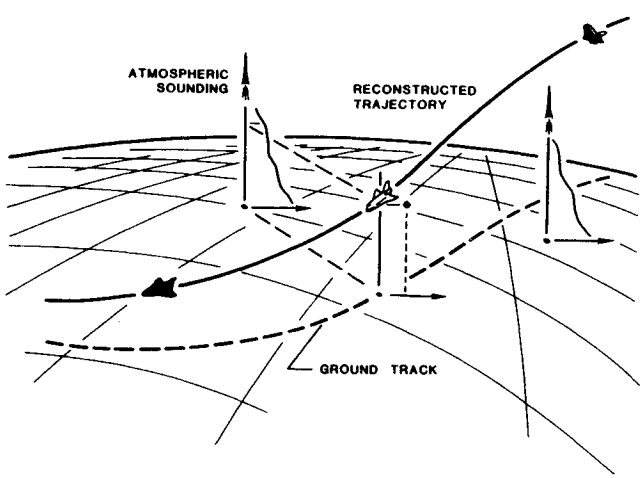

Fig. 6 Entry atmospheric reconstruction.

The results of the trajectory and atmospheric reconstruction processes are melded together to provide the best estimate of trajectory, which is an analytically and physically consistent definition of the freestream flight environment (i.e., freestream pressure, temperature, and density, wind-relative velocity, and angles of attack and sideslip) from near-orbital altitude to landing.

Aerodynamic Force and Moment Data

Inertial Measurement Units

The inertial measurement units (IMUs) are part of the Orbiter's operational instrumentation system. The triply redundant IMUs comprise all-attitude, four-gimbal, inertially stabilized platforms on which are mounted two mutually perpendicular linear accelerometers. In addition to the inertial acceleration data, primary outputs of the IMUs are vehicle velocity and attitude in the inertial reference space. Angular rate data may be inferred from the IMU attitude outputs.

Detailed descriptions of the IMU and other Orbiter operational systems can be found in Ref. 15.

Aerodynamic Coefficient Identification Package

Although the Orbiter's operational instrumentation system includes instruments that measure each of the vehicle motion parameters required for in-flight aerodynamic coefficient determination, these components were designed to meet only the operational requirements of vehicle guidance, navigation, and control. The measurement resolution and the data sampling rates of these instruments are not sufficient for accurate, research-quality determination of in-flight aerodynamic stability and control characteristics. Consequently, the Aerodynamic Coefficient Identification Package (ACIP) experiment[16] was designed specifically to enable collection of vehicle motion information with the resolution and data sampling rates required for accurate flight determination of Orbiter aerodynamic characteristics.

The ACIP includes three-axis, orthogonal sets of linear accelerometers, angular accelerometers, and rate gyros. The ACIP linear accelerometers operate over a measurement range of ±3 *g*, with a measurement resolution of 300 micro-*g*, which enables the ACIP to accurately measure vehicle motion data at altitudes below approximately 80 km. Thus, the ACIP experiment obtains data that are synergistic with those of the SEADS.

In addition to processing data from its own sensors, ACIP data-handling electronics also process control surface position sensor information for the Orbiter's four elevons and rudder, as well as operation data for a single aft RCS yaw thruster. These data are routed through the ACIP data-handling electronics to assure that they are recorded with proper time correlation, relative to the ACIP data, and at data rates that are sufficient to enable postflight estimation of vehicle stability and control characteristics. ACIP data are digitized to 14-bit resolution and recorded on the OEX recorder at a sampling rate of 174 Hz, as compared with the 1–25 Hz sampling rate range for similar operational instrumentation data.

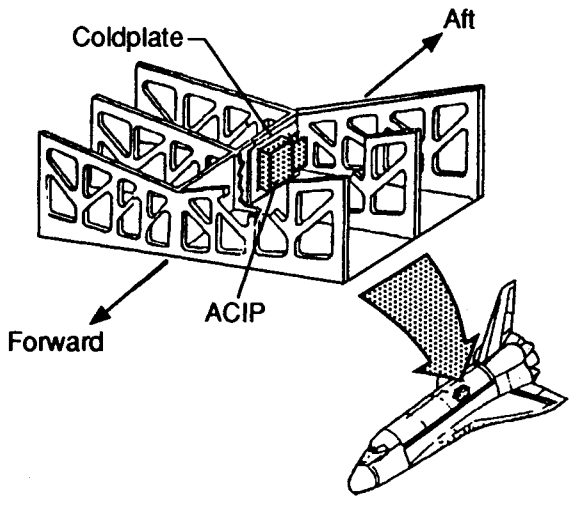

Fig. 7 ACIP installation schematic.

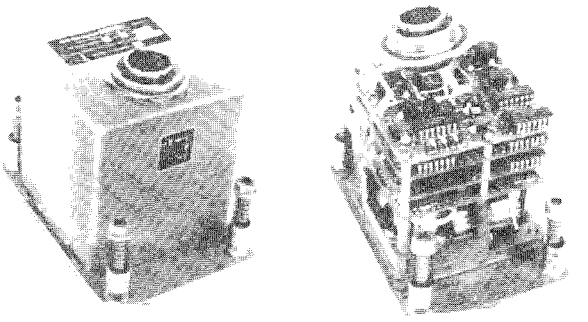

Fig. 8 HiRAP flight unit.

The ACIP is mounted on the Orbiter keel (Fig. 7), in the wing carrythrough structure beneath the payload bay, at a longitudinal position of approximately 76% of vehicle length. This location is about 315 cm aft (10% of vehicle length) and 216 cm below the Orbiter's entry center of gravity (c.g.). Proximity to the center of gravity minimizes the significance of correction factors associated with translation of the information for reference to the vehicle c.g. The ACIP is precisely aligned with respect to the Orbiter's body-axis coordinate system.

Two ACIP flight units were fabricated for use on the Orbiters Columbia and Challenger. An ACIP has flown on every flight of these two vehicles.

High-Resolution Accelerometer Package

The High-Resolution Accelerometer Package (HiRAP) experiment[17] comprises a three-axis, orthogonal set of high-resolution linear accelerometers. The HiRAP instrument operates over a range of ±8000 micro-*g*, with a measurement resolution of 1 micro-*g* and data sampling rate of 174 Hz. The measurement range of the HiRAP enables it to sense aerodynamic forces acting on the Orbiter from approximately 80 km to near-orbital altitudes. HiRAP data were intended to be obtained in conjunction with SUMS freestream density data, enabling direct determination (based solely on in situ measurements) of the aerodynamic performance characteristics of the Orbiter in the rarefied-flow flight regime.

The HiRAP (Fig. 8) is located beside the ACIP in the Orbiter's wing carrythrough structure, approximately 330 cm aft and 188 cm below the Orbiter's c.g., and is precisely aligned with respect to the Orbiter's body-axis coordinate system.

As with ACIP, two HiRAP flight units were fabricated for flight on the Orbiters Columbia and Challenger. A HiRAP unit has flown on eight missions of Challenger, beginning with its first flight (STS-6), and five missions of Columbia beginning with STS-9.[18]

Orbital Acceleration Research Experiment

The Orbital Acceleration Research Experiment[19] (OARE) complements the ACIP and HiRAP instruments by extending the altitude range over which vehicle aerodynamic acceleration data may be obtained to orbital altitudes. Like the HiRAP, the OARE instrument comprises a three-axis, orthogonal set of extremely sensitive linear accelerometers. The OARE instrument can be operated over three auto-selected, or preprogrammed, measurement ranges. The least-sensitive measurement range envelops that of the HiRAP instrument, the most sensitive range (±150 micro-*g*) is almost two orders of magnitude more sensitive than the HiRAP. On the most sensitive range, the measurement resolution of the OARE instrument is less than 5 nano-*g*. The operational range of the OARE is at such a low acceleration level that the sensors cannot be accurately calibrated in the 1-*g* ground environment. Consequently, the instrument sensors are mounted, within the OARE, on a rotary calibration table that enables an accurate calibration to be performed on orbit in the absence of Earth's gravity.

The OARE instrument produces acceleration data at an effective data rate of 10 Hz. These raw data may be recorded on an onboard tape recorder for postflight processing and analysis. However, because the OARE was intended to measure the low-frequency, aerodynamic accelerations over long orbital time periods, the instrument has its own internal data processing and storage capability. The internal data processing software, which may be modified from flight to flight, currently uses a trimmed mean filter algorithm to extract the steady-state acceleration signal. The processed data are then recorded on an internal solid-state memory device at a sampling rate of 1/25 Hz.

Unlike other OEX experiments, the OARE is carried as Orbiter payload. It is mounted at the bottom of the payload bay envelope (Fig. 9), on a carrier plate attached to the Orbiter's keel. This places the instrument approximately 165 cm aft and 137 cm below the Orbiter's entry center of gravity. It is, of course, precisely aligned with respect to the Orbiter's body axes.

On its first flight, on STS-40 in June 1991, the OARE experienced significant hardware anomalies that limited the accuracy of the data collected. The data obtained on this mission did, however, demonstrate the capability of the OARE instrument to resolve the extremely low levels of aerodynamic acceleration experienced by the Orbiter at orbital altitudes.[20] The STS-40 instrument anomalies were resolved, the equipment was repaired, and the OARE was operated successfully on mission STS-50.

Aerodynamic Surface Data

Development Flight Instrumentation

During the Orbital Flight Test missions (STS-1 through -5), the Orbiter Columbia was equipped with a large complement of diagnostic instrumentation that was referred to as the Development Flight Instrumentation (DFI). DFI measurements were intended to provide the requisite data for postflight certification of Orbiter subsystems designs before the start of Orbiter operational missions. The DFI system was comprised of over 4500 sensors, associated data-handling electronics, and data recorder.

Included among the DFI and of particular interest to aerothermodynamic researchers were measurements of the Orbiter's aerodynamic surface temperature at over 200 surface locations (Fig. 10). These measurements were obtained from thermocouples mounted within the TPS materials, in thermal contact with the TPS surface coatings.[21] The DFI also included temperature measurements in depth, within the TPS materials, at some 19 locations, and

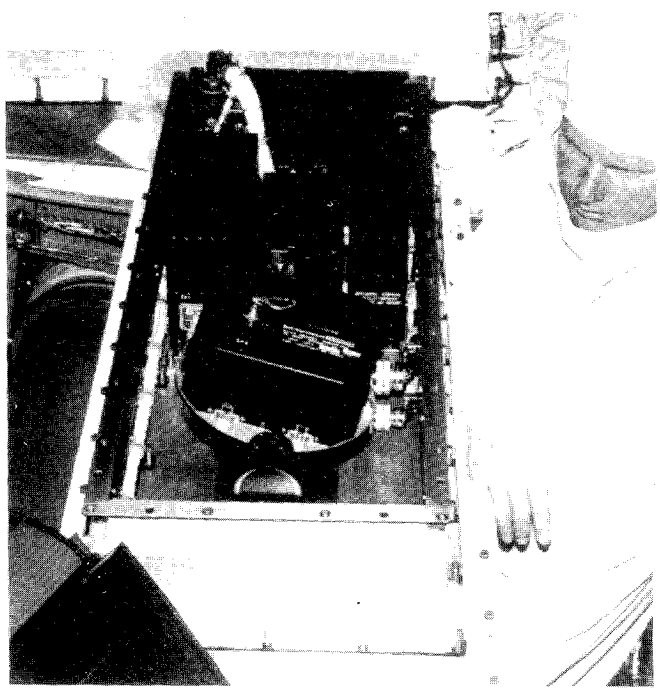

Fig. 9 OARE installed on Columbia for STS-40.

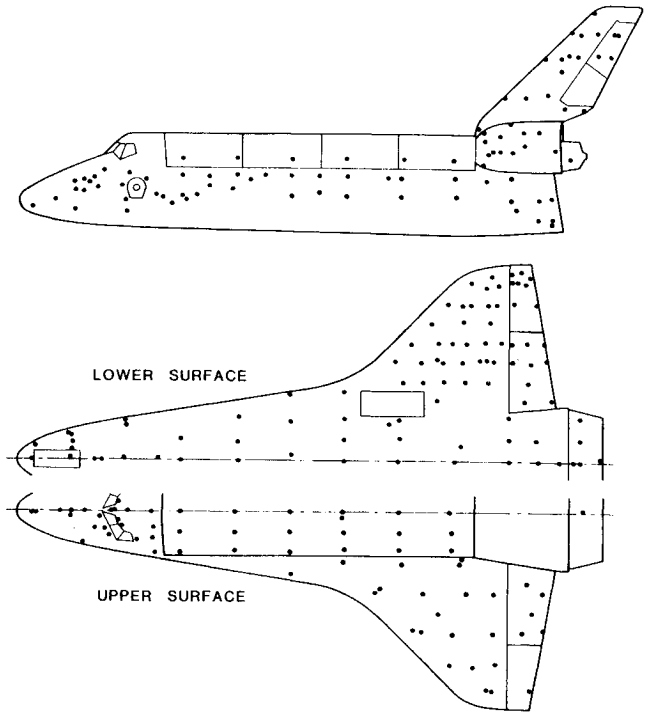

Fig. 10 DFI surface temperature measurement locations.

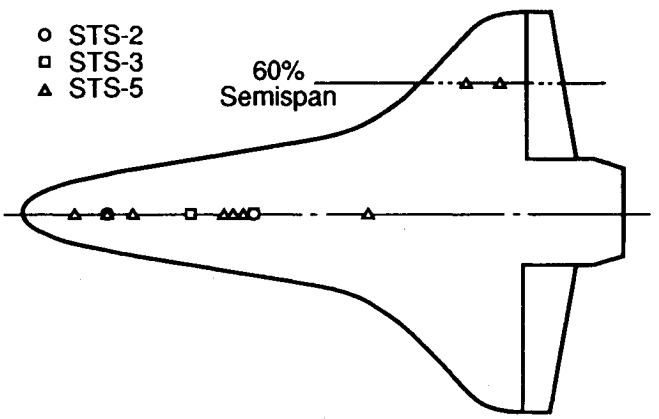

Fig. 11 CSE experiment coated tile locations.

along TPS tile sidewalls within the gaps between tiles at 16 locations. Aerodynamic surface pressure measurements were also made in numbers and distribution similar to the surface-temperature measurements.

The DFI were aboard Columbia on missions STS-1 through -5. However, mission-unique circumstances limited the amount of hypersonic entry temperature and pressure data collected on these flights. On missions STS-1 and -4, failures of the onboard flight data recorder precluded collection of data when the Orbiter was not in communications contact with a ground telemetry station. Consequently, data from these flights are available only for flight conditions of approximately Mach 12 and below. On STS-2, the pressure instrumentation was not "powered up" during entry. This was due to a constrained Orbiter entry power budget on this mission, which resulted from an in-flight failure of one of the Orbiter's three fuel cells. Pressure data were obtained over the complete entry trajectory only on missions STS-3 and -5, and temperature data were obtained over the complete entry trajectory only on missions STS-2, -3, and -5.

The DFI-derived surface temperature data from STS-2, -3, and -5 have been processed to infer aerodynamic heat transfer rates, using the methodology described in Ref. 22.

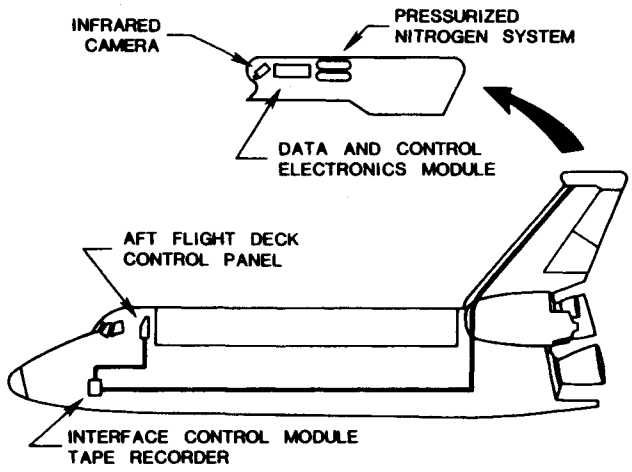

a) Schematic

b) SILTS pod atop vertical tail of Columbia

Fig. 12 SILTS experiment system.

Catalytic Surface Effects Experiment

Early arc jet testing of Orbiter thermal protection materials indicated that the reaction-cured glass (RCG) coating of the TPS tiles was noncatalytic to the recombination of dissociated air (specifically oxygen). Were this to be the case in flight, substantially reduced heat transfer levels could be expected, when compared with those that would be experienced if the surface were fully catalytic. Before the advent of Shuttle flights, however, this noncatalytic surface phenomenon had not been demonstrated to occur in the flight environment. Consequently, the Shuttle TPS design was predicated on the conservative assumption that the gas chemistry at the TPS surface would be in chemical equilibrium. The Catalytic Surface Effects (CSE) experiment[23] was conceived to provide direct confirmation of the noncatalytic nature of the TPS tile surface in flight and provide information with which to estimate, quantitatively, the catalytic efficiency of the RCG material.

The CSE experiment would provide an "inverse" demonstration of the noncatalytic nature of the baseline tile surface material. The implementation of this experiment involved coating selected Orbiter lower surface TPS tiles, which contained DFI surface temperature sensors, with a material that was known (based on arcjet tests) to be highly catalytic to the recombination of dissociated air. By comparing the flight-measured temperatures of the coated tiles and nearby baseline tiles, the relative catalytic efficiency of the baseline tile coating material would be demonstrated.

CSE experiment data were obtained on missions STS-2, -3, and -5.[24,25] On STS-2, two individual tiles on the lower surface centerline at 15 and 40% of vehicle length were coated (Fig. 11). For STS-3, individual tiles at 30 and 40% of vehicle length were coated. On STS-5, the catalytic coating was applied to individual tiles on the centerline at 10, 15, 20, 30, and 60% and continuously along a centerline strip from 35 to 40% of vehicle length. Two additional tiles, located at 76 and 82% of vehicle length along the 60% semispan chord of the wing were also coated.

Tile Gap Heating Experiment

The Tile Gap Heating (TGH) experiment[26] was intended to obtain entry flight data with which to investigate the phenomenon of aerodynamic heating in the gaps between adjacent thermal protection system tiles. The experiment hardware consisted of a carrier panel of tiles that was installed on the Orbiter's lower surface near the centerline at approximately 27% of vehicle length. This carrier panel bolted directly to the Orbiter structure and carried 11 tiles. At three locations on the array, tiles were instrumented with thermocouples in depth, on the outer tile surface, and along the sidewalls of the tile-to-tile gaps. Data from these thermocouples were recorded as part of the DFI system.

The experiment tiles were fabricated and installed with exacting specifications applied to the values of tile edge radius and gap width. The experiment plan was to systematically vary these parameters over multiple flights of the experiment panel to gain an understanding of the effects of these variables on tile gap heating and ultimately to determine optimum values of these parameters to minimize gap heating.

The TGH experiment was only flown on the STS-2 mission. Results from that flight are reported in Ref. 26.

Infrared Imagery of Shuttle Experiment

The objective of the Infrared Imagery of Shuttle (IRIS) experiment was to determine the temperature distribution over the Orbiter's lower surface at a *single* entry flight condition, at greater spatial resolution than would be achieved with the DFI measurements. This measurement was to be made remotely, by underflying the entering Orbiter with the NASA C-141 Kuiper Airborne Observatory (KAO) aircraft. An infrared image of the Orbiter would be obtained as it passed through the field of view of the KAO's astronomical telescope, which was equipped with two linear focal-plane arrays of infrared detectors.[27]

The IRIS experiment was successful in obtaining a partial image of the Orbiter on STS-3. Unfortunately, the image was found to be severely spatially and thermally distorted, and efforts to accurately resolve the image were unsuccessful.[27] As a result of extensive image data and experiment system analyses, the most likely cause of the distortion was determined to be atmospheric density gradients that existed in the open telescope cavity of the KAO aircraft. Consequently, it was concluded that a spatially resolvable image of the Orbiter was not attainable using this experimental technique.

Shuttle Infrared Leeside Temperature Sensing Experiment

The Shuttle Infrared Leeside Temperature Sensing (SILTS) experiment[28] was designed to obtain high-spatial-resolution temperature measurements of the leeside (wing and fuselage) of the Orbiter during entry. These measurements were obtained by means of an imaging, infrared radiometer (camera) located in a unique experiment pod atop the vertical tail of the Orbiter Columbia (Fig. 12). The SILTS camera contained a single infrared detector element and dual rotating scanning prisms (one horizontal and one vertical), which enabled the detector to scan the field of view, producing two-dimensional imagery. The experiment could be configured to view the Orbiter leeside surfaces through either of two infrared-transparent windows: one enabled viewing of the left wing, and the other enabled viewing of the fuselage.

The SILTS experiment pod also contained a data and control electronics module and a pressurized nitrogen system. Window protection plugs protected the viewport windows during Orbiter

ground handling, launch, and orbital operations. At experiment initiation, the window protection plugs were ejected, allowing the camera to "see" the Orbiter surfaces. The viewport windows were transpiration cooled during experiment operation by the injection of gaseous nitrogen over the external window surfaces. Active cooling of the windows was required to prevent window temperatures from increasing to levels at which the windows themselves would become radiators in the infrared, thus "fogging" the data images.

On a normal mission, the SILTS experiment was initiated at the time the Orbiter reached the "entry interface" altitude of 122 km, and infrared imagery was collected throughout the hypersonic portion of atmospheric entry. A data image was obtained approximately every 8.6 s during experiment operation. SILTS data were recorded on the OEX flight data recorder.

The SILTS experiment was flown on five Orbiter missions. Significant SILTS hardware anomalies prevented useful data from being obtained on its first flight on STS-61C.[29] Useful data were obtained, however, on four subsequent flights. Flights of the SILTS experiment on STS-28[30] and -32 provided temperature data for the Orbiter's left wing throughout the hypersonic portion of entry. The experiment was configured to view the leeside fuselage on the STS-35 and -40 missions. Unique operational anomalies occurred on each of these flights (different for each flight), which limited the quantity of data obtained. Nevertheless, valuable fuselage temperature data were obtained[31] over constrained portions of the entry trajectory as indicated in Fig. 13.

Aerothermal Instrumentation Package

The Aerothermal Instrumentation Package (AIP) comprised some 125 measurements of aerodynamic surface temperature and pressure at discrete locations on the leeside of the Orbiter's left wing, side and upper fuselage, and vertical tail (Fig. 14). AIP temperature sensors provided in situ measurements that constituted both "ground-truth" and corollary information for the SILTS

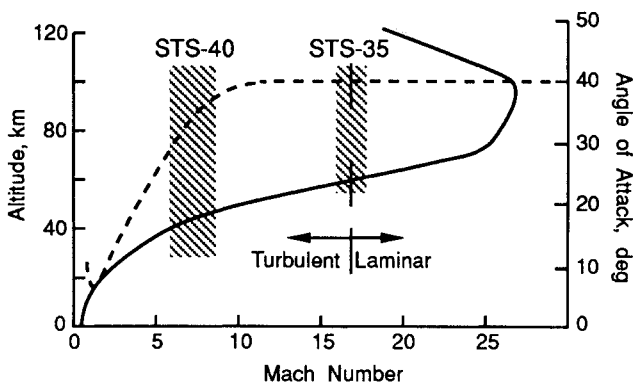

Fig. 13 SILTS fuselage data availability.

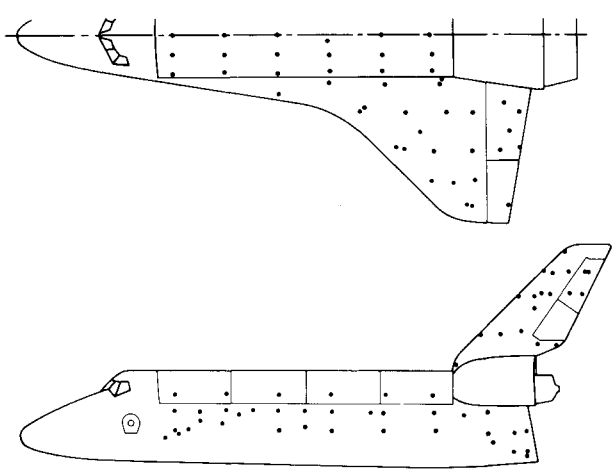

Fig. 14 AIP surface temperature measurement locations.

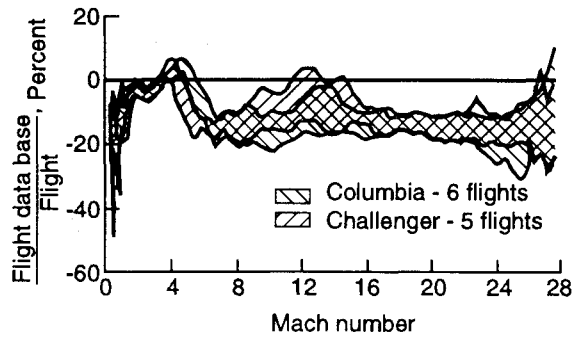

Fig. 15 Comparison of flight-measured and preflight-predicted axial-force coefficients (adapted from Ref. 32).

experiment. The AIP pressure sensors were intended to provide data to support investigations of reaction control system jet interactions with the aerodynamic flowfield.

All of the AIP sensors were originally elements of the DFI system. They were reactivated through implementation of new Orbiter wire harnesses that connected the sensors to an AIP-unique data-handling system. Temperature and pressure data were recorded at sampling rates of 5.3 and 21.3 Hz, respectively, on the OEX flight data recorder.

AIP data were obtained throughout the hypersonic portion of atmospheric entry on Shuttle missions STS-28, -32, and -40. Only limited data (below about 73 km altitude) were obtained on STS-35, the result of a ground telemetry failure, which also affected the SILTS experiment.

Vehicle Configuration Data

Orbiter control surface position data are measured and recorded in flight by elements of the Orbiter's operational instrumentation system. As was discussed in the preceding section on the ACIP, certain of these data are also processed, in parallel, by the ACIP data-handling electronics. Operational measurements of control surface positions are recorded at rates of 1–25 Hz.

Reaction control system thruster firing data are inferred by measurements of pressure in the jet combustion chambers. These data are recorded at the rate of 25 Hz.

Vehicle mass, center of gravity, and moments of inertia are determined analytically by means of a complex mass accounting system. Each Orbiter was weighed to establish a baseline set of mass and center-of-gravity information. A database of mass and location information is maintained for all additional Orbiter hardware and other elements (e.g., payloads) that may be installed on, or removed from, the Orbiter vehicle during ground processing. During flight, consumables are continually monitored. Using this mass accounting system, a history of vehicle mass properties is produced following each flight.

OEX Experiment Flight-Test Results

Flights of OEX experiment instrumentation aboard the Orbiters Columbia and Challenger have provided a wealth of hypersonic aerothermodynamic flight data. These data have been, and are continuing to be, used in research analyses with the objectives of 1) improving our understanding of the hypersonic flight environment and 2) advancing the state of the art of methodologies to be used for predicting the aerothermodynamic characteristics of advanced space transportation vehicles. The following subsections provide a sampling (by no means an exhaustive list) of results that have emanated from some of the research analyses performed to date, using these data.

Orbiter Aerodynamic Performance

Included among the information required for, or resulting from, the derivation of the best estimate of trajectory are all of those data required to determine the values of parameters that describe the Orbiter's aerodynamic performance characteristics. These parameters include lift-to-drag ratio; lift-, drag-, and side-force coeffi-

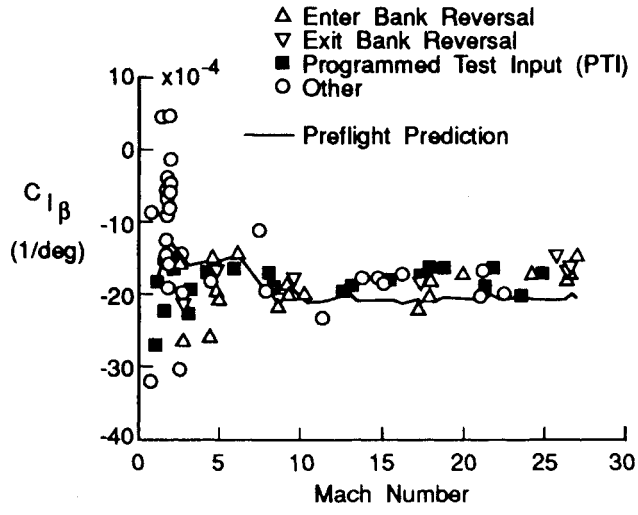

Fig. 16 Comparison of flight-measured and preflight-predicted coefficients of rolling moment due to sideslip (adapted from Ref. 33).

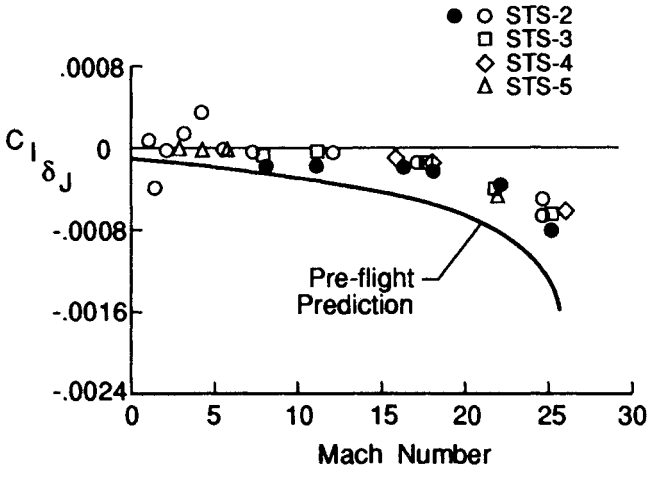

Fig. 17 Comparison of flight-measured and preflight-predicted coefficients of rolling moment due to yaw jet (adapted from Ref. 34).

cients; as well as pitching-, yawing-, and rolling-moment coefficients. Flight values of these aerodynamic performance parameters have been derived for multiple Orbiter entries and compared with the wind-tunnel-derived preflight aerodynamic design data.[32] Figure 15 contains a typical comparison, this between the flight-derived and preflight-predicted data for the axial-force coefficient.

Orbiter Stability and Control

Beginning with the second Shuttle flight and continuing to the present, aerodynamic maneuvers have been executed during entry specifically to obtain Orbiter stability and control data. These maneuvers, referred to as programmed test inputs (PTIs), have been designed to provide the data required for determination of specific stability and control parameters.[33] Execution of these maneuvers is accomplished by direct input to the flight control system through onboard software. The amplitude and timing of control surface motions are governed by programmed variables that generate specific control inputs at predesignated flight conditions. Vehicle response data are measured by the ACIP. After flight, the aerodynamic stability and control parameters are determined by analyses of the maneuvers using the maximum likelihood estimation process just described. A typical example of flight-measured stability and control data (in this case, rolling moment due to sideslip) compared with preflight predictions is presented in Fig. 16.

Reaction Control System—Aerodynamic Flowfield Interactions

Because of interactions between reaction control jet plumes and the Orbiter's aerodynamic flowfield, RCS jet firings during entry

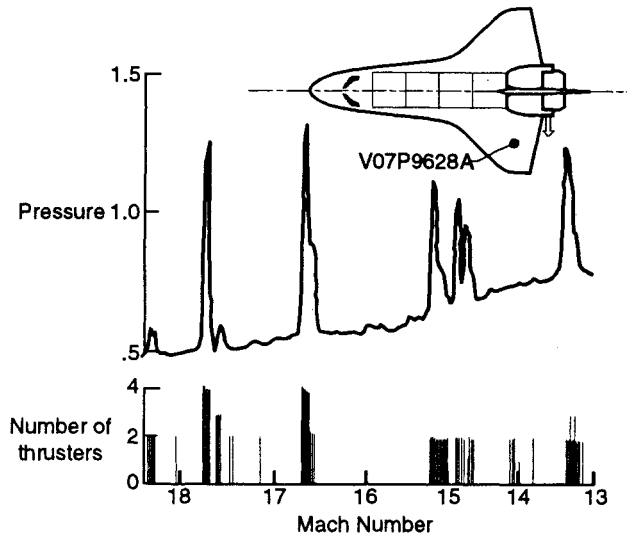

Fig. 18 Effect of RCS yaw jet firings on wing upper surface pressure (adapted from Ref. 34).

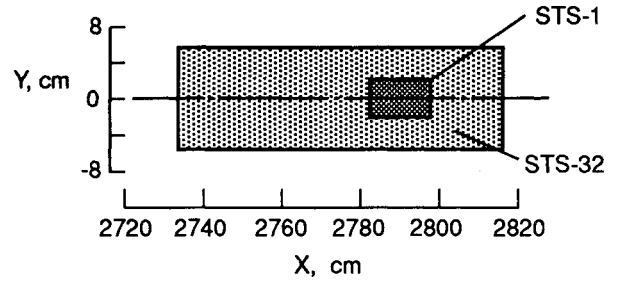

Fig. 19 Expansion of Orbiter allowable center-of-gravity envelope (courtesy of D. B. Kanipe, NASA Johnson Space Center).

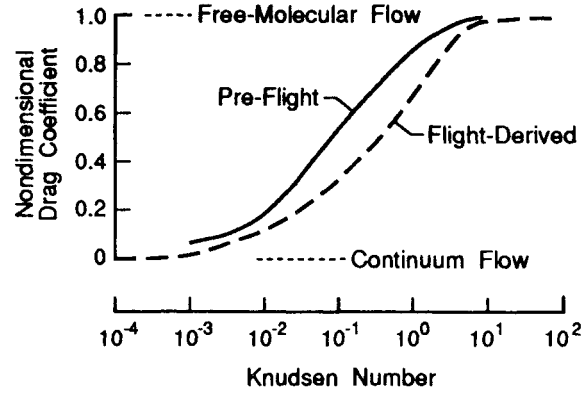

Fig. 20 Comparison of preflight and flight-derived rarefied-flow aerodynamic bridging formulas (adapted from Ref. 35).

may *not* result in control forces and moments that are in direct proportion to the thrust of the RCS jet. The adequacy of ground-test modeling of these interactions and the accuracy of the resultant interaction data were of significant concern before the STS-1 mission. Aerodynamic stability and control parameters associated with RCS jet firings are determined from flight data in the same manner as described in the preceding section: firing of an RCS jet is simply treated as a control input. Flight-derived RCS aerodynamic interaction data indicated that some of the interactions were not well simulated in the preflight ground-based testing. As an example, Fig. 17 presents a comparison of the flight-derived and preflight predicted data for rolling moment due to yaw jet firing.

Scallion et al.[34] demonstrated that the interaction component of the forces or moments resulting from an RCS jet firing could be determined directly from measured aerodynamic surface pressure

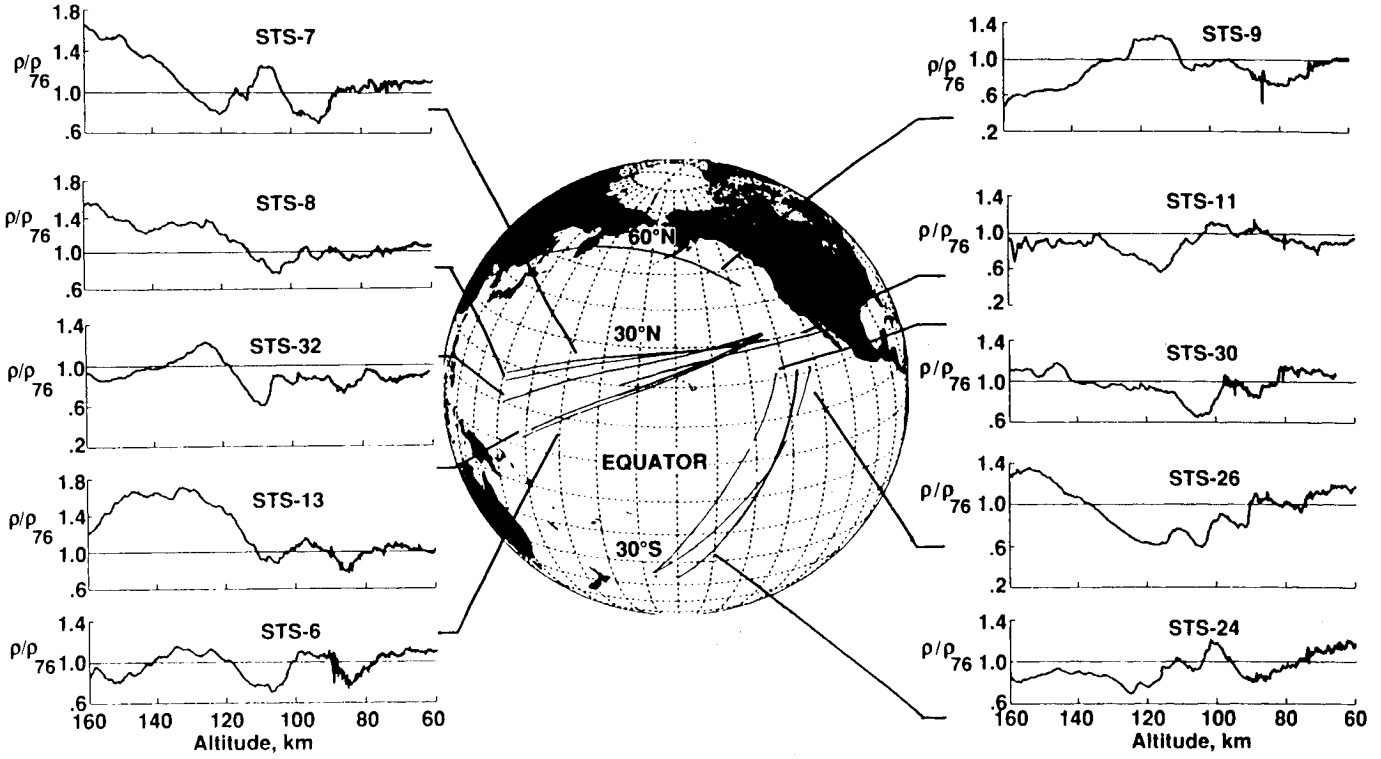

Fig. 21 Flight-derived atmospheric density data above 60 km (adapted from Ref. 36).

data. The magnitude of the RCS plume aerodynamic interaction was determined by evaluating the differences between surface pressures measured with RCS jets ON and jets OFF (Fig. 18) and then integrating the delta pressures over the aerodynamic surfaces. Demonstration of this approach to measurement of RCS aerodynamic interactions has led to further research focused on improved techniques for simulating these interactions in ground-based facilities.

Orbiter Allowable Center-of-Gravity Envelope

The preflight uncertainties associated with the Orbiter's aerodynamic performance and stability and control characteristics were reflected in a highly constrained allowable center-of-gravity envelope for STS-1. Indeed, on STS-1, significant ballast was carried on the vehicle to attain the desired c.g. location. As a direct result of the determination of the Orbiter's in-flight aerodynamic characteristics, using data obtained by the ACIP, the aerodynamic uncertainty levels have been continually reduced. Reduced aerodynamic performance and control uncertainties have, in turn, resulted in significant expansion of the allowable c.g. envelope for Orbiter operations. This is illustrated in Fig. 19, which compares the STS-1 allowable c.g. envelope with that for STS-32. The expanded c.g. envelope affords significantly increased flexibility in the configuration of payload bay cargos as the requirements for orbiter c.g. control are decreased.

Transitional-Flow Aerodynamic Bridging Formula

In the absence of Orbiter experimental aerodynamic data in the transitional-flow regime, an aerodynamic bridging formula was used to infer the aerodynamic performance of the vehicle at flight conditions where the flowfield surrounding the vehicle could *not* be considered continuum in nature. Data obtained in hypersonic wind tunnels were used to describe the vehicle's continuum-flow aerodynamic performance. Free-molecular-flow calculations were used to define aerodynamic performance at flight conditions where the free-molecular assumption was deemed appropriate (assumed for Knudsen number greater than 10). A bridging formula was used to interpolate between these limits to define the Orbiter's aerodynamic performance at the intermediate altitudes, which

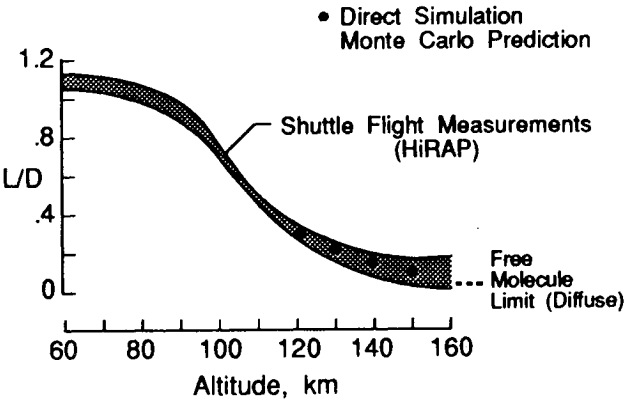

Fig. 22 Comparison of DSMC aerodynamic predictions with flight data (adapted from Ref. 37).

were assumed to represent flight conditions where the flowfield would be transitional in nature.

The pre-STS-1 bridging formula assumed a $\sin^2$ function in Knudsen number to describe the aerodynamic force coefficients between continuum and free-molecular "anchor points." This $\sin^2$ functional form had its heritage in the blunt-body work of the Apollo era. Flight measurements of Orbiter aerodynamic forces obtained by the HiRAP experiment, however, indicated that this bridging formula did *not* accurately predict the Orbiter's aerodynamic performance characteristics in the transitional-flow regime. The blunt-body-based bridging formula was not appropriate for application to a lifting vehicle.

The flight-measured aerodynamic data have been used in the development of an improved bridging formula,[35] which is applicable to lifting vehicles. This new bridging formula is functionally an exponential in Knudsen number and provides a substantially different prediction of rarefied-flow aerodynamic performance than the blunt-body-based formula (Fig. 20). Additionally, it not only compares well with the flight data (from which it was derived) but also compares well with data obtained in ground-based facilities over the Mach number range of 10–25.[35]

High-Altitude Atmospheric Density Variability

Atmospheric density information for the altitude range of 60–160 km has been derived, for multiple entries, using the accelerometry data obtained by the HiRAP and IMU instruments.[36] Unlike standard atmospheric profiles that indicate atmospheric parameter variations only in the vertical, the Orbiter-derived profiles were obtained over large horizontal ranges. Consequently, imbedded within these profiles are data that may provide insights into the latitudinal, longitudinal, and local solar time variations of atmospheric density. Typical flight-derived density data, normalized by the 1976 standard atmosphere values, are shown as a function of altitude in Fig. 21. The flight-derived density profiles display significant wavelike variations, relative to the standard atmosphere, which appear to be random from flight to flight. The difference between measured and standard model densities, for any given flight and altitude, may be significant (in excess of 50%).

Direct Simulation Monte Carlo Validation

Direct Simulation Monte Carlo (DSMC) is a state-of-the-art computational technique for simulating flowfields about vehicles operating in the transitional- and rarefied-flow flight regimes. Comparisons have been made between DSMC predictions and HiRAP-measured flight data, for Orbiter lift-to-drag (L/D) ratio over the altitude range of 120–170 km.[37] The DSMC results and the flight data were in excellent agreement (Fig. 22). In the DSMC simulation, the molecule surface interaction model assumed full accommodation and diffuse reflection of molecules. The agreement between the DSMC predictions and the flight data suggests that in flight, at these altitudes, the interaction of gas molecules with the surface of the Orbiter's thermal protection materials is properly characterized as fully diffuse.

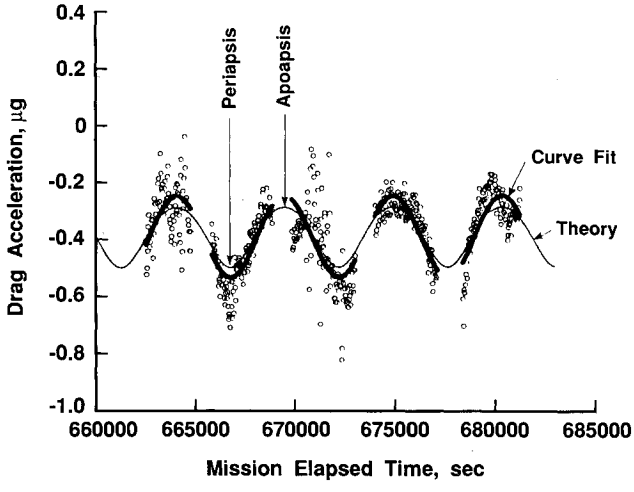

Fig. 23 Orbital drag variability measured by OARE on STS-40 (courtesy of R. C. Blanchard, NASA Langley Research Center).

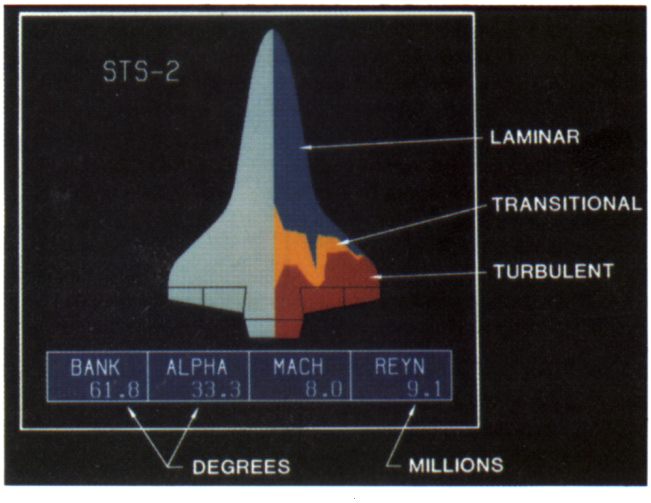

Fig. 24 Typical STS-2 boundary-layer transition contour plot.

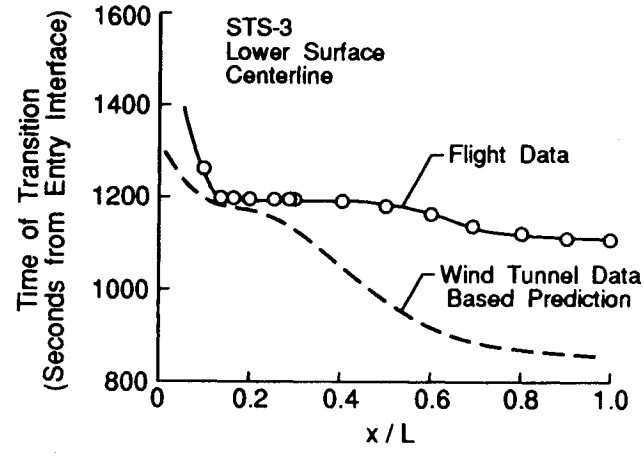

Fig. 25 Comparison of STS-3 flight data and preflight prediction for boundary-layer transition on the windward surface centerline (adapted from Ref. 40).

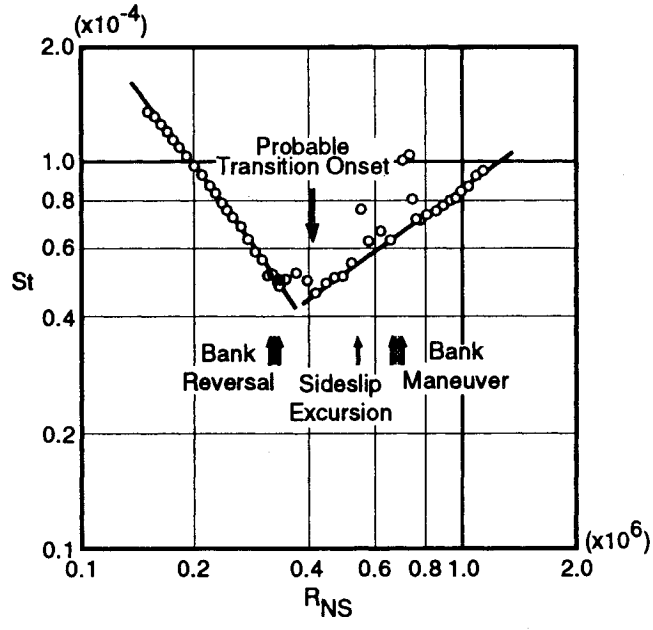

Fig. 26 STS-28 heat transfer to leeside centerline at $x/L=0.70$, angle of attack constant at 40 deg (adapted from Ref. 42).

Orbital Drag Variation

On its initial flight, the OARE experienced hardware anomalies that severely compromised the quantitative accuracy of the data obtained. However, the instrument's ability to sense the nano-g accelerations resulting from the aerodynamic drag of the Orbiter while on orbit was demonstrated.[38] The variation in measured drag acceleration level as a function of orbital period is illustrated in Fig. 23 for a time span of 3 1/2 orbits. The periodic drag variation about each orbit resulted primarily from changes in atmospheric density along the orbital track. These density changes were primarily due to vehicle altitude variations resulting from the elliptic nature of the orbit.

Windward Surface Boundary-Layer Transition

Temperature time histories derived from DFI thermocouple measurements provided the basis for determination of the time, during entry, of boundary-layer transition onset and completion at each windward surface measurement location. Hartung and

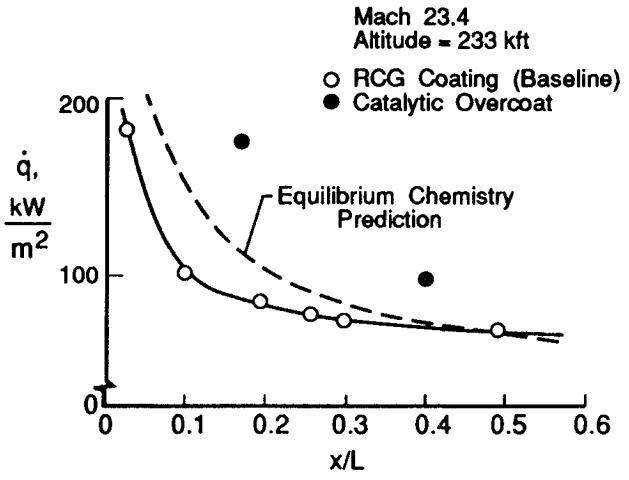

Fig. 27 CSE experiment results confirm the noncatalytic nature of the baseline RCG tile coating (derived from STS-2 CSE experiment data).

Throckmorton[39] created a database of this information and used these data to generate contour "maps" indicating the location and extent of the boundary-layer transition front for each time at which data were recorded (1 Hz). These transition contour maps (Fig. 24) were sequentially presented in a movie format to provide real-time visualization of the movement of the boundary-layer transition front during entry. The complexity of the transition contours and the abrupt (in time) manner in which they were observed to move strongly indicated that the in-flight transition process was dominated by the effects of discrete surface roughness elements.

Goodrich et al.[40] compared the flight-observed transition along the windward centerline with preflight predictions derived using a methodology based on wind-tunnel test results. This methodology attempted to account for the potential effects of surface roughness by comparing the wind-tunnel results obtained with both smooth and roughened surface models. In flight, boundary-layer transition occurred much later than predicted over the aft 75% of the vehicle's centerline whereas the predictions and flight results were in fairly good agreement along the forward 25% of the centerline (Fig. 25). The differences in predicted vs actual transition times, over the aft portion of the vehicle, were attributed to acceleration of the transition process in the wind tunnel as a result of tunnel noise, which is, of course, *not* present in the flight environment. The favorable agreement over the forward portion of the vehicle was attributed to surface roughness domination of the transition process in this region, *both* in the wind tunnel and in flight.

Leeside Shock-Layer Transition

Analysis of leeside heat transfer data[41] revealed the occurrence of an unexpected transition in the Orbiter's leeside flowfield in flight, which was not observed in the wind tunnel. This transition was indicated by a sudden increase in surface heat transfer observed simultaneously at multiple locations on the leeside fuselage and wing. It has been postulated[42] that this transition occurs in the shear layer downstream of lines of flow separation that exist along the vehicle's forward fuselage and wing leading edges. Thus, it is not a localized phenomenon but rather a "global" phenomenon that, once initiated, rapidly affects the entire leeside shock layer. Lee and Harthun[43] noted that, in wind-tunnel tests, no differences were observed in leeside heating data obtained with or without boundary-layer trips located on the nose of Orbiter models to induce turbulence in the leeward flowfield. They concluded that "either the turbulent flow relaminarized when it expanded to the leeward side, or the flow on the leeward side was turbulent without the trips."

Figure 26 presents typical flight heat transfer data that illustrate the data trends that are indicative of leeside shock-layer transition onset. Although not indicated in the data of Fig. 26, transition of the leeside flowfield in flight is apparently "incipient" over a narrow portion of the entry flight regime and may be "tripped" as a result of disturbances to the leeside flowfield structure that accompany small, transient perturbations to the vehicle's nominal flight attitude.[42]

Since leeside shock-layer transition occurs at much higher Reynolds number conditions in flight than in the wind tunnel, leeside heat transfer data obtained in hypersonic wind tunnels *may not* accurately reflect flight heat transfer levels at the higher altitude, lower Reynolds number conditions, when the flight leeside shock layer is laminar. Transition in the leeside shock layer is *not* related to windward surface boundary-layer transition. The leeside phenomenon occurs at approximately Mach 16, whereas windward side boundary-layer transition occurs in the Mach 8–10 range.[39,40]

TPS Surface Catalytic Efficiency

The Catalytic Surface Effects experiment successfully demonstrated that the surface of the Orbiter's thermal protection system tiles was substantially noncatalytic to the recombination of dissociated oxygen atoms.[24,25] This result is illustrated in Fig. 27.

In-flight contamination of several instrumented tiles provided a further serendipitous demonstration of the noncatalytic nature of the baseline TPS surface on missions STS-2 and -3.[44] On these missions, sudden "jumps" in surface temperature were observed (Fig. 28) at several measurement locations, apparently as the result of instantaneous change of the catalytic efficiency of the TPS surface. This change in surface catalytic efficiency resulted from sur-

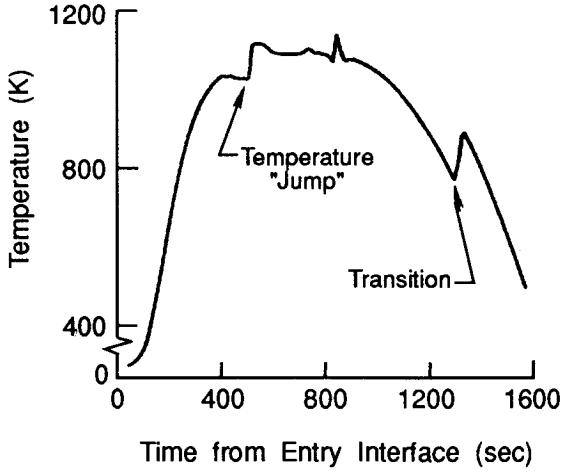

Fig. 28 STS-2 temperature-time history data for the windward centerline at $x/L=0.194$ (adapted from Ref. 44).

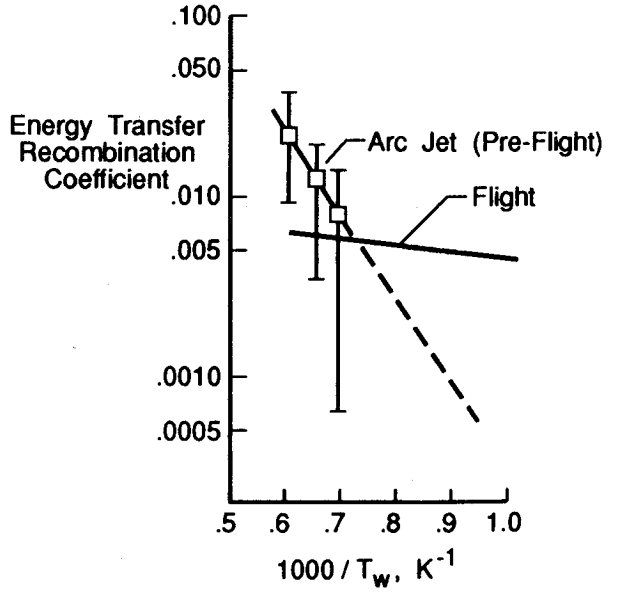

Fig. 29 Comparison of arcjet and flight-derived energy recombination coefficients for baseline TPS tile surface (adapted from Ref. 46).

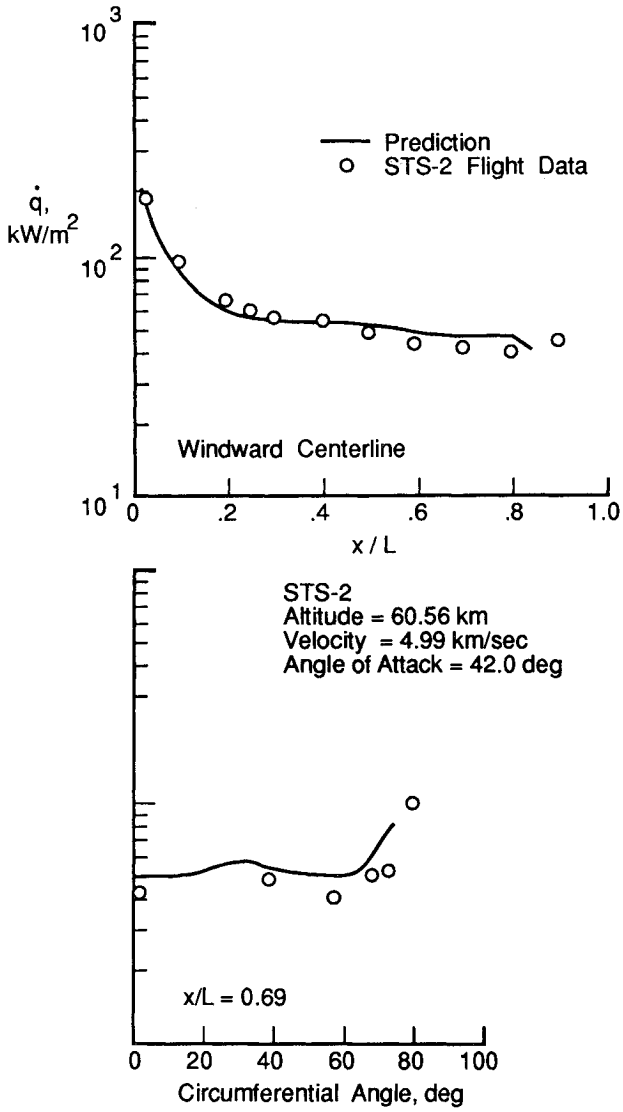

Fig. 30 Comparison of DFI flight data with predictions of a state-of-the-art, three-dimensional, viscous shock-layer computational technique (adapted from Ref. 47).

face deposition of highly catalytic oxidation products from a melting, upstream sensor cover. The event apparently occurred when the stainless steel sensor cover's temperature reached the level at which it began to oxidize, thereby allowing contaminants to be carried downstream. As with the design of the CSE experiment, the increased heating due to the contamination confirmed the noncatalytic nature of the baseline TPS surface material.

TPS Surface Recombination Rate Coefficients for Oxygen

The prediction of surface heat transfer rates in a chemically reacting flow over a surface that is not fully catalytic requires adequate modeling of the gas surface interaction chemistry. For Shuttle entry, the predominant surface reaction of interest is the recombination of dissociated oxygen atoms. Before the collection of Orbiter entry flight data, the only available recombination reaction rate data were those inferred from measurements of heat transfer to Shuttle thermal protection system tiles in ground-based arcjet tests.[45] These experimental data were measured at wall temperature levels (>1400 K) significantly above the temperature range (800–1400 K) actually experienced by Orbiter TPS tiles during entry; consequently, their application to predictions of Orbiter entry heat transfer levels required significant extrapolation.

Windward centerline heat transfer data obtained over a constrained altitude range (71–78 km) on STS-2 were used as benchmarks for the determination of flight-derived surface recombination rate data.[46] An axisymmetric viscous shock-layer technique, capable of modeling the finite rate reacting gas chemistry both in the flowfield and at the body surface, was used to compute the heat transfer to the Orbiter's windward centerline. In these computations, the surface reaction rate coefficients for oxygen were treated as independent variables and varied parametrically. Comparisons of the computational results with the STS-2 flight data allowed determination of those reaction rate coefficients that provided the best fit to the measured flight data and thus defined a new expression for the temperature-dependent reaction rate coefficients.[46] This expression is graphically compared with the previous arcjet data in Fig. 29. Use of this recombination rate expression for prediction of heat transfer at other flight conditions (i.e., altitudes other than the 71–78 km altitude range from which the benchmark data were obtained) and on other missions resulted in prediction of heating rates to within approximately 10% of the flight-measured values[46] for the Orbiter's windward centerline.

Computational Fluid Dynamic Technique Validation

DFI Data Comparisons

The entry heat transfer data derived from DFI temperature measurements constitute benchmark hypersonic flight results. These data have been used extensively for comparison with the results of various computational methods for simulating the flowfield structure about, and resulting heat transfer to, hypersonic flight vehicles. The predictive techniques have ranged from simplified engineering methods, which may only treat the vehicle windward centerline and be limited to perfect gas or equilibrium chemistry, to fully three-dimensional Navier-Stokes solutions, with modeling of the finite rate, reacting gas chemistry.

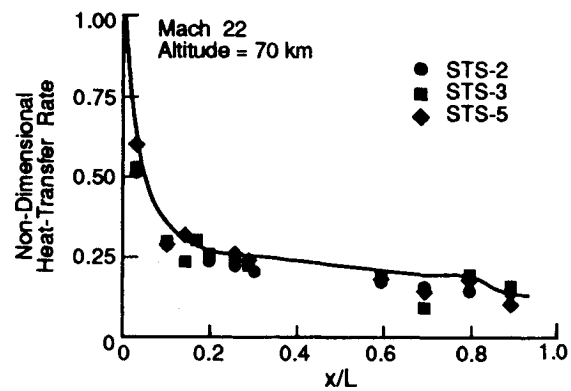

a) Windward centerline

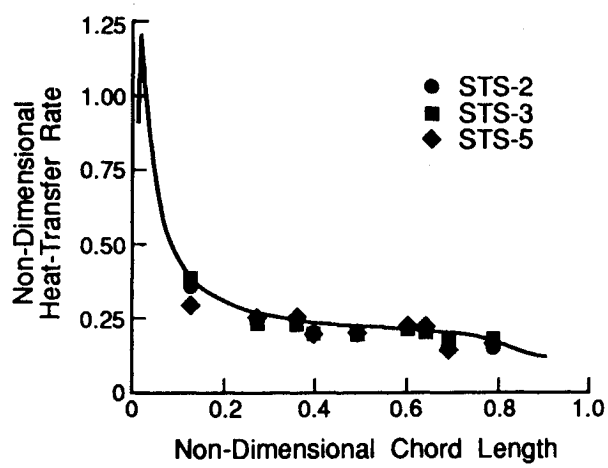

b) Wing chord at 50% semispan

Fig. 31 Comparison of DFI flight data with predictions of a state-of-the-art, three-dimensional, Navier-Stokes computational technique (adapted from Ref. 48).

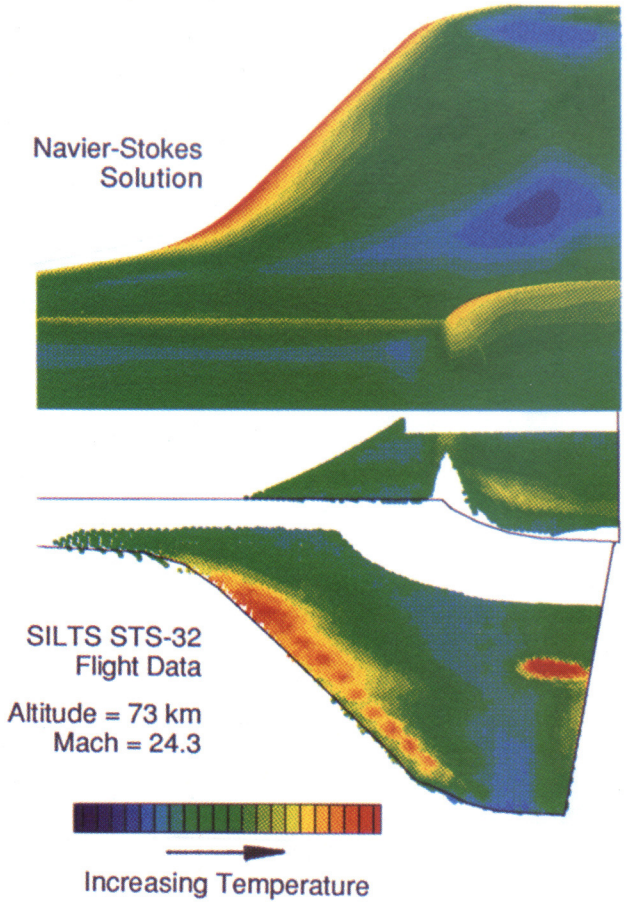

Fig. 32 Comparison of SILTS flight data with predictions of a state-of-the-art, three-dimensional, Navier-Stokes computational technique (adapted from Ref. 49).

Two recent sets of comparisons are particularly noteworthy as examples of the use of the flight data for validation of state-of-the-art computational fluid dynamic (CFD) methods. These CFD solutions were obtained for a modified Orbiter geometry that provided an accurate representation of the Orbiter's windward surface; however, the complex Orbiter leeside geometry was replaced with a simplified shape. The modified shape of the leeside geometry had no effect on the windward surface flowfield calculations, since both the streamwise and crossflow components of velocity are supersonic near the leading edges.

Thompson[47] presented surface heat transfer predictions obtained using a three-dimensional, viscous shock-layer technique, including consideration of the nonequilibrium flowfield chemistry and finite wall catalytic efficiency. Wall temperatures were specified, based on the flight-measured temperatures along the windward centerline. Figure 30 shows typical comparisons between the flight data and computed results for the vehicle windward centerline and spanwise at 69% of vehicle length.

Weilmuenster and Gnoffo[48] presented surface heat transfer predictions obtained using a three-dimensional Navier-Stokes code, again including consideration of the nonequilibrium flowfield chemistry and finite wall catalytic efficiency. In this calculation, the wall temperature was computed based on a radiation-equilibrium model. Figure 31 presents typical comparisons between the flight data and computed results for the windward centerline and a wing chord at 50% of the vehicle semispan.

SILTS Data Comparison

Kleb and Weilmuenster[49] assessed the ability of a state-of-the-art computational method to accurately simulate the flowfield, and resulting heat transfer, over the leeside of the Orbiter during entry. Using the same computational technique cited in Ref. 48, a solution was obtained over the complete Shuttle Orbiter. The computational geometry was an accurate representation of the actual Shuttle Orbiter, as far aft as the location of the body-flap hinge line. The only simplifications made to the geometry definition were omission of the body flap, the Shuttle main engines, and the vertical tail.

The solution results were compared with both the discrete location data obtained with DFI thermocouples and the full-surface, high-spatial-resolution data obtained by the SILTS experiment. The comparison between the SILTS data and the computational results is shown in Fig. 32.

Concluding Remarks

Space Shuttle operations have provided recurring opportunities for the study of entry aerothermodynamic phenomena unique to lifting entry vehicles in hypersonic flight. The NASA Orbiter Experiments Program capitalized on that opportunity by the development and operation of unique instrumentation specifically designed to obtain Orbiter aerothermodynamic flight data during atmospheric entry. In this manner, the Shuttle Orbiter has been used as an entry flight research vehicle as an adjunct to its normal operational mission. The information derived from the OEX experiments, as well as baseline Orbiter instrumentation, represents heretofore unavailable benchmark hypersonic flight data. These data are being used in a continual process of validation of state-of-the-art methods, both experimental and computational, for simulating and/or predicting the aerothermodynamic flight characteristics of advanced space transportation vehicles.

Acknowledgments

Although those individuals responsible for the OEX experiments described herein have, by and large, been recognized by reference to their published work, the author wishes to specifically recognize each of the past and present principal (or co-) investigators for the OEX aerothermodynamic experiments; SEADS: P. M. Siemers III, NASA Langley Research Center; SUMS: R. C. Blanchard, NASA Langley Research Center; ACIP: D. R. Cooke and D. B. Kanipe, NASA Johnson Space Center; HiRAP: R. C. Blanchard, NASA Langley Research Center; OARE: R. C. Blanchard, NASA Langley Research Center; CSE: D. A. Stewart, NASA Ames Research Center; TGH: W. C. Pitts, NASA Ames Research Center; IRIS: W. C. Davy, M. J. Green, and B. L. Swenson, NASA Ames Research Center; SILTS: J. C. Dunavant, D. A. Throckmorton, and E. V. Zoby, NASA Langley Research Center; and AIP: D. A. Throckmorton, NASA Langley Research Center.

No OEX experiment could have been successfully flown were it not for the untiring efforts of the personnel of the OEX Project Office at the NASA Johnson Space Center. The OEX Project Office was responsible for overall OEX Project management, management and engineering interfaces with the Shuttle Orbiter Project, provision of an OEX data handling/recording system, assurance of OEX experiment flight operational planning and control, and integration of all OEX experiment systems aboard the Orbiter. The personnel of the OEX Project Office, who were a part of the OEX Team during the 15-year life span of this project, are no less deserving of recognition than the experiment principal investigators and their hardware support teams. However, the numbers of people involved preclude their individual acknowledgment. Nevertheless, they know who they are! They should know that they have the gratitude of this author and each of the principal investigators whose research benefited substantially as a result of their efforts.

References

[1]Anon., "Executive Summary," *NASA Office of Aeronautics and Space Technology Summer Workshop*, NASA TM X-73960, Aug. 1975.

[2]Anon., "Entry Technology," *NASA Office of Aeronautics and Space Technology Summer Workshop*, Vol. 9, NASA TM X-73969, Aug. 1975.

[3]Hayes, W. C., Jr., "OAST Shuttle Orbiter Experiments Program," Testimony before the Subcommittee on Space Science and Applications, Committee on Science and Technology, United States House of Representatives, Feb. 9, 1977.

[4]Iliff, K. W., "Parameter Estimation for Flight Vehicles," *Journal of Guidance, Control, and Dynamics*, Vol. 12, No. 5, 1989, pp. 609–622.

[5]Siemers, P. M., III, and Larson, T. J., "Space Shuttle Orbiter and Aerodynamic Testing," *Journal of Spacecraft and Rockets*, Vol. 16, No. 4, 1979, pp. 223–231.

[6]Jones, J. J., "OEX—Use of the Shuttle Orbiter as a Research Vehicle," AIAA Paper 81-2512, Nov. 1981.

[7]Throckmorton, D. A., "Research Analysis of Space Shuttle Orbiter Entry Aerothermodynamic Flight Data at the NASA Langley Research Center," AIAA Paper 81-2429, Nov. 1981.

[8]Cary, J. P., and Keener, E. R., "Flight Evaluation of the X-15 Ball-Nose Flow-Direction Sensor as an Air Data System," NASA TN D-2923, July 1965.

[9]Pruett, C. D., Wolf, H., Heck, M. L., and Siemers, P. M., III, "Innovative Air Data System for the Space Shuttle Orbiter," *Journal of Spacecraft and Rockets*, Vol. 20, No. 1, 1983, pp. 61–69.

[10]Siemers, P. M., III, Wolf, H., and Henry, M. W., "Shuttle Entry Air Data System (SEADS)—Flight Verification of an Advanced Air Data System Concept," AIAA Paper 88-2104, May 1988.

[11]Blanchard, R. C., Duckett, R. J., and Hinson, E. W., "The Shuttle Upper Atmosphere Mass Spectrometer Experiment," *Journal of Spacecraft and Rockets*, Vol. 21, No. 2, 1984, pp. 202–208.

[12]Moss, J. N., and Bird, G. A., "Monte Carlo Simulations in Support of the Shuttle Upper Atmosphere Mass Spectrometer Experiment," *Journal of Thermophysics and Heat Transfer*, Vol. 2, No. 2, 1988, pp. 138–144.

[13]Compton, H. R., Findlay, J. T., Kelly, G. M., and Heck, M. L., "Shuttle (STS-1) Entry Trajectory Reconstruction," AIAA Paper 81-2459, Nov. 1981.

[14]Price, J. M., "Atmospheric Definition for Shuttle Aerothermodynamic Investigations," *Journal of Spacecraft and Rockets*, Vol. 20, No. 2, 1983, pp. 133–140.

[15]Anon., "National Space Transportation System Reference," NASA TM-101,877, June 1988.

[16]Anon., "End Item Specification—Aerodynamic Coefficient Identification Package (ACIP) and High Resolution Accelerometer Package (HiRAP) for Shuttle Orbiter Experiments," The Bendix Communications Division, Aerospace Systems Operations, Specification 3291583, Ann Arbor, MI, Dec. 1981.

[17]Blanchard, R. C., and Rutherford, J. F., "Shuttle Orbiter High Resolution Accelerometer Package Experiment: Preliminary Flight Results," *Journal of Spacecraft and Rockets*, Vol. 22, No. 4, 1985, pp. 474–480.

[18]Blanchard, R. C., Larman, K. T., and Barrett, M., "The High Resolution Accelerometer Package (HiRAP) Flight Experiment Summary for the First Ten Flights," NASA RP-1267, March 1992.

[19]Blanchard, R. C., Hendrix, M. K., Fox, J. C., Thomas, D. J., and Nicholson, J. Y., "Orbital Acceleration Research Experiment," *Journal of Spacecraft and Rockets*, Vol. 24, No. 6, 1987, pp. 504–507.

[20]Blanchard, R. C., Nicholson, J. Y., and Ritter, J. R., "STS-40 Orbital Acceleration Research Experiment Flight Results During a Typical Sleep Period," NASA TM-104209, Jan. 1992.

[21]Stoddard, L. W., and Draper, H. L., "Development and Testing of Development Flight Instrumentation for the Space Shuttle Orbiter Thermal Protection System," *Proceedings of the 24th International Symposium*, Instrument Society of America, Albuquerque, NM, May 1978.

[22]Throckmorton, D. A., "Benchmark Determination of Shuttle Orbiter Entry Aerodynamic Heat-Transfer Data," *Journal of Spacecraft and Rockets*, Vol. 20, No. 3, 1983, pp. 219–224.

[23]Stewart, D. A., Rakich, J. V., and Lanfranco, M. J., "Catalytic Surface Effects Experiment on the Space Shuttle," *Thermophysics of Atmospheric Entry*, edited by T. E. Horton, Vol. 82, Progress in Astronautics and Aeronautics, AIAA, New York, 1982, pp. 248–272.

[24]Rakich, J. V., Stewart, D. A., and Lanfranco, M. J., "Results of a Flight Experiment on the Catalytic Efficiency of the Space Shuttle Heat Shield," AIAA Paper 82-944, June 1982.

[25]Stewart, D. A., Rakich, J. V., and Lanfranco, M. J., "Catalytic Surface Effects on Space Shuttle Thermal Protection System During Earth Entry of Flights STS-2 Through STS-5," *Shuttle Performance: Lessons Learned*, NASA CP-2283, Pt. 2, March 1983, pp. 827–845.

[26]Pitts, W. C., and Murbach, M. S., "Flight Measurements of Tile Gap Heating on the Space Shuttle," AIAA Paper 82-0840, June 1982.

[27]Green, M. J., Budnik, M. P., Yang, L., and Chaisson, M. P., "Supporting Flight-Data Analysis for Space-Shuttle Orbiter Experiments at NASA Ames Research Center," NASA TM 84345, April 1983.

[28]Throckmorton, D. A., Zoby, E. V., and Kantsios, A. G., "The Shuttle Infrared Leeside Temperature Sensing (SILTS) Experiment," AIAA Paper 85-0328, Jan. 1985.

[29]Dunavant, J. C., Myrick, D. L., Zoby, E. V., and Throckmorton, D. A., "Shuttle Infrared Leeside Temperature Sensing (SILTS) Experiment—STS 61-C Final Results," NASA TP-2958, Dec. 1989.

[30]Throckmorton, D. A., Zoby, E. V., Dunavant, J. C., and Myrick, D. L., "Shuttle Infrared Leeside Temperature Sensing (SILTS) Experiment—STS-28 Preliminary Results," AIAA Paper 90-1741, June 1990.

[31]Throckmorton, D. A., Zoby, E. V., Dunavant, J. C., and Myrick, D. L., "Shuttle Infrared Leeside Temperature Sensing (SILTS) Experiment—STS-35 and STS-40 Preliminary Results," AIAA Paper 92-0126, Jan. 1992.

[32]Findlay, J. T., Kelly, G. M., Heck, M. L., and McConnell, J. G., "Final Report: Summary of Shuttle Data Processing and Aerodynamic Performance Comparisons for the First Eleven (11) Flights," NASA CR-172440, Sept. 1984.

[33]Cooke, D. R., "Minimum Testing of the Space Shuttle Orbiter for Stability and Control Derivatives," *Shuttle Performance: Lessons Learned*, NASA CP-2283, Part 1, March 1983, pp. 447–472.

[34]Scallion, W. I., Compton, H. R., Suit, W. T., Powell, R. W., Blackstock, T. A., and Bates, B. L., "Space Shuttle Third Flight (STS-3) Entry RCS Analysis," AIAA Paper 83-0116, Jan. 1983.

[35]Blanchard, R. C., and Buck, G. M., "Rarefied Flow Aerodynamics and Thermosphere Structure from Shuttle Flight Measurements," *Journal of Spacecraft and Rockets*, Vol. 23, No. 1, 1986, pp. 18–24.

[36]Blanchard, R. C., Hinson, E. W., and Nicholson, J. Y., "Shuttle High Resolution Accelerometer Package Experiment Results: Atmospheric Density Measurements Between 60–160 km," *Journal of Spacecraft and Rockets*, Vol. 26, No. 3, 1989, pp.173–180.

[37]Bird, G. A., "Application of the Direct Simulation Monte Carlo Method to the Full Shuttle Geometry," AIAA Paper 90-1692, June 1990.

[38]Blanchard, R. C., Nicholson, J. Y., and Ritter, J. R., "STS-40 Orbital Acceleration Research Experiment Flight Results During a Typical Sleep Period," NASA TM 104209, Jan. 1992.

[39]Hartung, L. C., and Throckmorton, D. A., "Computer Graphic Visualization of Orbiter Lower-Surface Boundary-Layer Transition," *Journal of Spacecraft and Rockets*, Vol. 24, No. 2, 1987, pp. 109–114.

[40]Goodrich, W. D., Derry, S. M., and Bertin, J. J., "Shuttle Orbiter Boundary Layer Transition at Flight and Wind Tunnel Conditions," *Shuttle Performance: Lessons Learned*, NASA CP-2283, Pt. 2, March 1983, pp. 753–780.

[41]Throckmorton, D. A., and Zoby, E. V.: "Orbiter Entry Leeside Heat-Transfer Data Analysis," *Journal of Spacecraft and Rockets*, Vol. 20, No. 6, 1983, pp. 524–530.

[42]Throckmorton, D. A., "Leeside Shock-Layer Transition and the Space Shuttle Orbiter," *Journal of Spacecraft and Rockets* (to be published).

[43]Lee, D. B., and Harthun, M. H., "Aerothermodynamic Entry Environment of the Space Shuttle Orbiter," *Entry Vehicle Heating and Thermal Protection Systems: Space Shuttle, Solar Starprobe, Jupiter Galileo Probe*, edited by P. E. Bauer and H. E. Collicott, Vol. 85, Progress in Astronautics and Aeronautics, AIAA, New York, 1983, pp. 3–20.

[44]Throckmorton, D. A., Zoby, E. V., and Hamilton, H. H., II, "Orbiter Catalytic/Non-Catalytic Heat Transfer as Evidenced by Heating to Contaminated Surfaces on STS-2 and STS-3," *Shuttle Performance: Lessons Learned*, NASA CP-2283, March 1983, pp. 847–864.

[45]Scott, C. D., "Catalytic Recombination of Nitrogen and Oxygen on High-Temperature Reusable Surface Insulation," *Aerothermodynamics of Planetary Entry*, edited by A. L. Crosbie, Vol. 77, Progress in Astronautics and Aeronautics, AIAA, New York, 1981, pp. 192–213.

[46]Zoby, E. V., Gupta, R. N., and Simmonds, A. L., "Temperature-Dependent Reaction Rate Expressions for Oxygen Recombination," *Thermal Design of Aeroassisted Orbital Transfer Vehicles*, edited by H. F. Nelson, Vol. 96, Progress in Astronautics and Aeronautics, AIAA, New York, 1985, pp. 445–464.

[47]Thompson, R. A., "Comparison of Viscous-Shock-Layer Solutions with Shuttle Heating Measurements," *Journal of Thermophysics and Heat Transfer*, Vol. 4, No. 2, pp. 162–169.

[48]Weilmuenster, K. J., and Gnoffo, P. A., "A Solution Strategy for Three-Dimensional Configurations at Hypersonic Speeds," *Journal of Spacecraft and Rockets* (to be published).

[49]Kleb, W. L., and Weilmuenster, K. J., "Characteristics of the Shuttle Orbiter Leeside Flow During a Reentry Condition," *Journal of Spacecraft and Rockets* (to be published).